ELSEVIER

Biochimica et Biophysica Acta 1228 (1995) 1–27

BBA Biochimica et Biophysica Acta

Review

Forces and factors that contribute to the structural stability of membrane proteins

Tuomas Haltia, Ernesto Freire *

Department of Biology and Biocalorimetry Center, The Johns Hopkins University, Baltimore, MD 21218, USA

Received 30 June 1994; accepted 17 October 1994

Keywords: Calorimetry; Thermal stability; Bacteriorhodopsin; Cytochrome oxidase; Band 3 protein; Photosystem II

Contents

1. Summary

While a considerable amount of literature deals with the structural energetics of water-soluble proteins, relatively little is known about the forces that determine the stability of membrane proteins. Similarly, only a few membrane protein structures are known at atomic resolution, although new structures have recently been described. In this article, we review the current knowledge about the structural features of membrane proteins. We then proceed to summarize the existing literature regarding the thermal stability of bacteriorhodopsin, cytochrome-*c* oxidase, the band 3

* Corresponding author. Fax: +1 (410) 5166469.

SSDI 0005-2728(94)00161-8

protein, Photosystem II and porins. We conclude that a fundamental difference between soluble and membrane proteins is the high thermal stability of intrabilayer secondary structure elements in membrane proteins. This property manifests itself as incomplete unfolding, and is reflected in the observed low enthalpies of denaturation of most membrane proteins. By contrast, the extramembranous parts of membrane proteins may behave much like soluble proteins. A brief general account of thermodynamics factors that contribute to the stability of water soluble and membrane proteins is presented.

2. Introduction

Biological membranes are essential to living organisms as they provide a selective permeability barrier and also the environment for a multitude of functional processes. The membranes are composed of lipid and protein molecules in an approximately equal proportion on a weight basis, even though deviations are known to occur [68]. The lipid molecules define a highly fluid bilayer that serves as an anchoring matrix for the protein molecules. The protein molecules, on the other hand, are traditionally divided into two main classes: some of them contain a significant portion of their mass within the interior of the membrane (intrinsic or integral membrane proteins) while other proteins are only associated to the surface of the membrane (extrinsic or peripheral membrane proteins). In this review, we will only consider integral membrane proteins in which the peptide traverses the bilayer one or more times. Peripheral membrane proteins, even though essential components of membranes, are actually water soluble proteins with a high affinity for a specific component on the membrane surface.

A lipid bilayer has a tripartite structure: the fatty acyl chains make up a 25–30 Å wide hydrophobic core that is flanked by the relatively polar headgroup regions measuring about 10–15 Å each. The bilayer is however a very dynamic structure and thermal fluctuations appear to impose a large effect on its thickness [238]. Thus it is not appropriate to consider a bilayer as a static hydrocarbon slab (for a review on the nature of lipid bilayer and peptide–bilayer interactions, see ref. [236]). The core has a dielectric constant close to that of liquid alkanes ($\epsilon = 2$), whereas the headgroup regions have an intermediate dielectric constant in the range of 10–30 [68]. For comparison, water has an ϵ of 80 while a typical protein interior is thought to have an ϵ of 3–5 [83]. Owing to the ester carbonyls and water associated to the lipid headgroups, lipid molecules are electrical dipoles which, when oriented as in a bilayer, give rise to a considerable electric potential (on the order of hundreds of mV), positive inside the bilayer [58,60,68]. This so-called dipole potential appears to be an inherent property of any lipid bilayer whether natural or man-made. Its presence may explain why a bilayer is generally far less permeable for a positive than for a negative ion. However, interaction of electrical membrane potential with positively charged side chains is thought to be the most important topological determinant of membrane proteins [6].

During the last decade a significant effort has been devoted to the elucidation of the mechanisms that control the folding and particularly the insertion and topological determinants of membrane proteins (see Refs. [33,44,49,50,92,117,128,150,156,157,163,164,210,215,224, 228,235,244,252] for recent accounts). As a result, the membrane topology of an α-helical multispanning membrane protein can often be predicted with relative accuracy from the primary structure of the protein [94,150,152, 194,226]; but see [252,256]. Much less is known about how the helices interact to make up the tertiary structure, although some features of this process are currently emerging [155]. Since membrane proteins have proven to be extremely difficult to crystallize or to study by other methods aimed at high resolution structure determination (for recent achievements see Refs. [105,153]), most topological information derives mainly from studies employing site-directed mutagenesis and biochemical assays as well as sequence analysis and structure prediction. Also, and contrary to the case of water soluble proteins, relatively little is known regarding the magnitude and relative importance of the forces that determine the structural stability of membrane proteins (cf. [36,39,244]). The purpose of this review is to summarize recent observations and advance some unifying principles regarding the structural stabilization of membrane proteins.

Unlike soluble proteins, intrinsic membrane proteins are designed to fold and exist in a milieu from which water is largely excluded. Since the magnitude of many of the forces involved in protein folding (e.g., hydrogen bonding, the hydrophobic effect and electrostatic interactions) is intimately coupled to the properties of the solvent, those forces are expected to play different roles in the stabilization of membrane proteins [157,164]. For example, the hydrophobic effect cannot directly drive tertiary structure formation within the lipid bilayer. Also, questions concerning matters such as the folding pathway or the formation and stability of secondary structure may have distinctly different answers in the case of membrane proteins. However, there is one field of structural research in which membrane proteins may offer an advantage over soluble proteins: prediction of secondary and tertiary structure from the amino acid sequence. This is the case because of the constraints imposed by the lipid bilayer on the possible folding schemes of a transmembrane protein, thus reducing the number of conformations accessible to the polypeptide (see, e.g., [50,228], but see also [117,252] and Section 3.2). In the case of some α-helical membrane proteins having only short extramembranous loops that limit the possible arrangement of the helices, the structure prediction problem reduces to a large extent to that of discriminating lipid facing residues from those facing other helices

[9,50,163,164,217]. A fully automated sequence-based prediction method for α-helical membrane proteins has been described [210].

To date, the stability of only a handful of membrane proteins, including cytochrome-*c* oxidase, bacteriorhodopsin, the band 3 protein from red blood cells and plant Photosystem II have been measured calorimetrically, providing a relatively small set of thermodynamic data. A common observation of these calorimetric studies is that the enthalpy change associated with the thermal denaturation of these molecules is smaller than the one found for water soluble proteins of similar molecular weight, suggesting that membrane proteins do not undergo complete thermal unfolding.

From a structural point of view, membrane proteins are composed of (i) regions that are exposed to the aqueous medium, (ii) regions that are in direct contact with the lipid components of the membrane and (iii) regions that face the protein interior, cofactors or other proteins that are either intrinsic or extrinsic (for an experimental method to define these regions, see [4]). In general, the proportion of protein mass exposed to the aqueous medium can be as small as 20–30% as in the case of bacteriorhodopsin [80] or as large as more than 90% as in the case of prostaglandin H synthase [153]. In some multisubunit membrane proteins such as cytochrome-*c* oxidase, some of the subunits are very hydrophobic and are likely to reside largely inside the bilayer while other subunits are rather hydrophilic and are located outside the lipid bilayer membrane. Owing to this promiscuous nature of membrane proteins, it is apparent that protein–protein as well as protein–lipid interactions and the hydration of amino acid residues need to be considered in order to account for their structural stability.

3. The structure of membrane proteins

3.1. Survey of structural features

The 3D structures of three non-related membrane proteins have been solved to atomic resolution, viz. structures of two bacterial reaction centers [3,26,45,55,100,128], four porins [32,104,233,234] and, very recently, prostaglandin H synthase [153,255]. The largely α-helical structure of bacteriorhodopsin has been determined at near atomic resolution (3.5 Å and 10 Å resolution in the parallel and perpendicular planes of the membrane, respectively) by using cryo-electron microscopy of 2D crystals [80]. The same technique has also been used to demonstrate helix movements associated with proton translocation during the photocycle of bacteriorhodopsin [207]. The structure of the plant light-harvesting complex at 3.4 Å resolution was recently determined with electron crystallography [105]. For a number of other membrane proteins, cryo-electron microscopy of 2D-crystals has yielded structural information at a resolution high enough to allow at least partial identification of secondary structure elements (Ca^{2+}-ATPase [214,256]; Photosystem I [102]; the band 3 protein [48,230]; halorhodopsin [78]; rhodopsin [181]; the nicotinic acetylcholine receptor [218]; the vacuolar H^+-ATPase proteolipid [56]). In the case of a bacterial chemoreceptor, where a major part of the protein makes up a peripheral water soluble domain, it has been possible to determine the structure of the soluble part by X-ray crystallography [129,189] and use that information together with results from other, less direct experiments to obtain a structural model of the whole protein [119,148,189]; for related studies on other proteins, see Refs. [1,13,47,220]. Similarly, the structure of the soluble portion of cytochrome *f* from the chloroplast b_6f complex has been recently determined at 2.3 Å resolution [34,125].

The transmembrane parts of both the bacterial reaction centers and bacteriorhodopsin are α-helical, in contrast to those of porins, which are almost 100% β-sheet proteins. Prostaglandin H synthase [153] appears to be an example of what was thought to be an unlikely folding pattern for a membrane protein, viz. a monotopic membrane protein [14,193] (see Fig. 1). This enzyme is mostly extramembranous and has four short amphipathic helices parallel to the membrane plane; these helices anchor the enzyme to the bilayer without traversing the whole membrane [153,255]. It is notable that this mode of interaction with the bilayer could not be predicted by sequence analysis [255]. In the lower resolution structures cited above, the predominant membrane-spanning element appears to be the α-helix; however, one should remember that β-sheet may be harder to identify by electron crystallography (cf. [71,117,218]). The determination of membrane protein secondary structures by using spectroscopic techniques is not always straightforward [33,57,218,247]. Thus, the apparent rarity of β-sheets among the currently known membrane protein structures may also reflect the limited size of the existing high resolution structural database. In fact, the transmembranous segment of the nicotinic acetylcholine receptor may be representative of a fourth membrane protein folding motif. The receptor transmembrane domain appears to comprise five central α-helices, one from each of the five homologous subunits, surrounded by a β-sheet barrel [71,218,247,252] (see Fig. 1f), a structure resembling the toxin fold found in two pentameric bacterial toxins [195,198]. Another example of intrabilayer β-structures might be provided by voltage-gated potassium channels in which an eight-stranded antiparallel β-barrel surrounded by 24 α-helices has been suggested to form the ion selective pore of the channel [51,154,252]. Each of the four subunits of the potassium channel is thought to contribute six helical segments and a β-sheet hairpin which forms part of the pore (see Fig. 1g). (Note that in this case the pore may not be in contact with lipids.)

3.2. The membrane spanning helix

The transmembrane α-helix is undoubtedly the best characterized structural element in membrane proteins. A

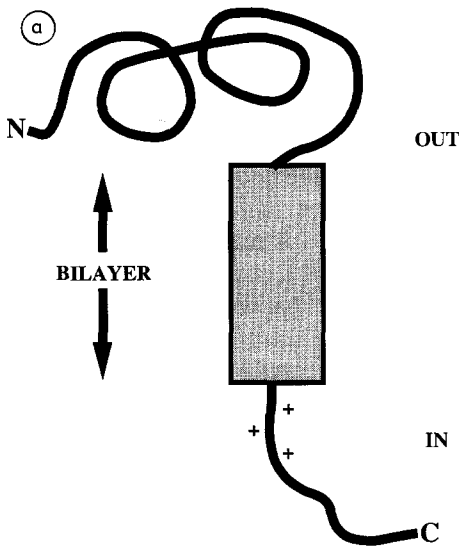

Type I

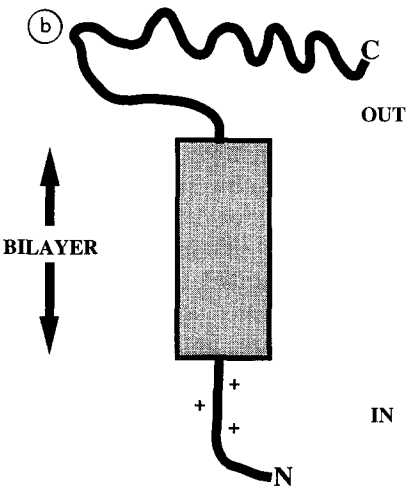

Type II

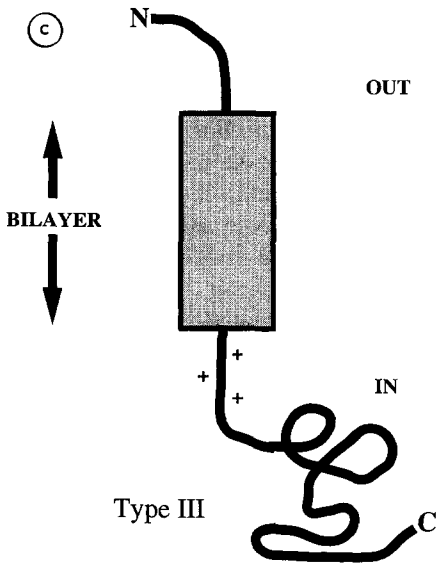

Type III

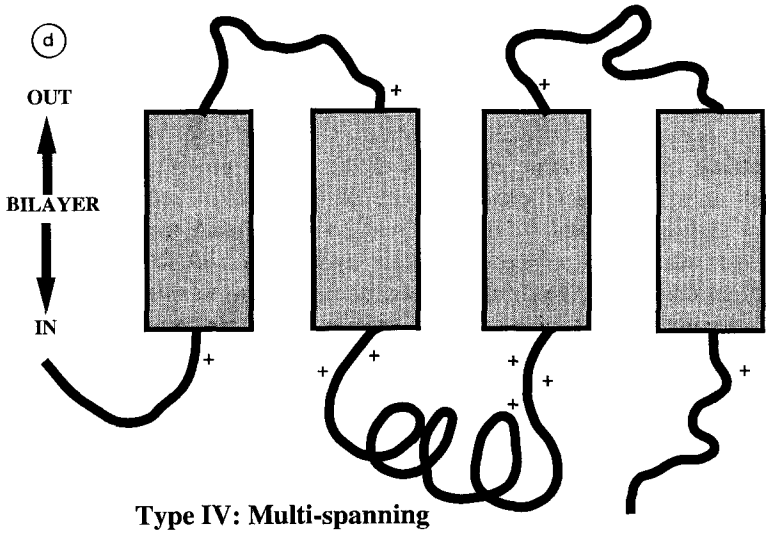

Type IV: Multi-spanning

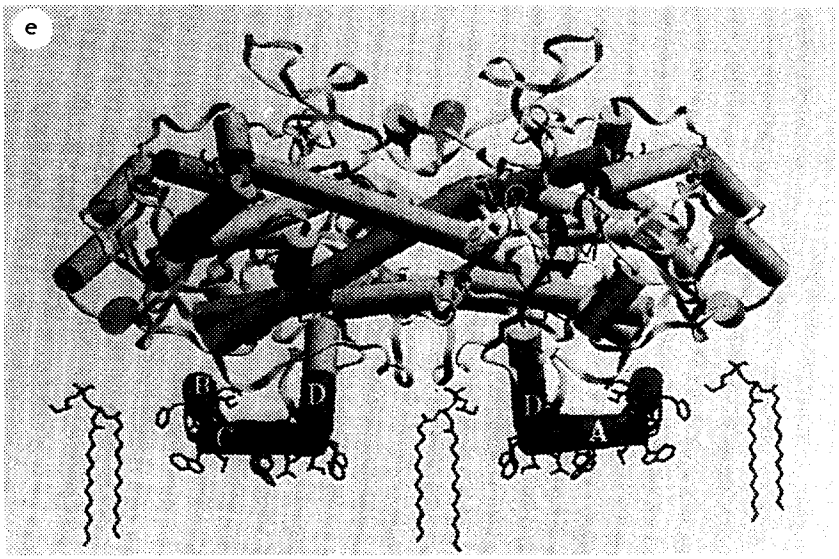

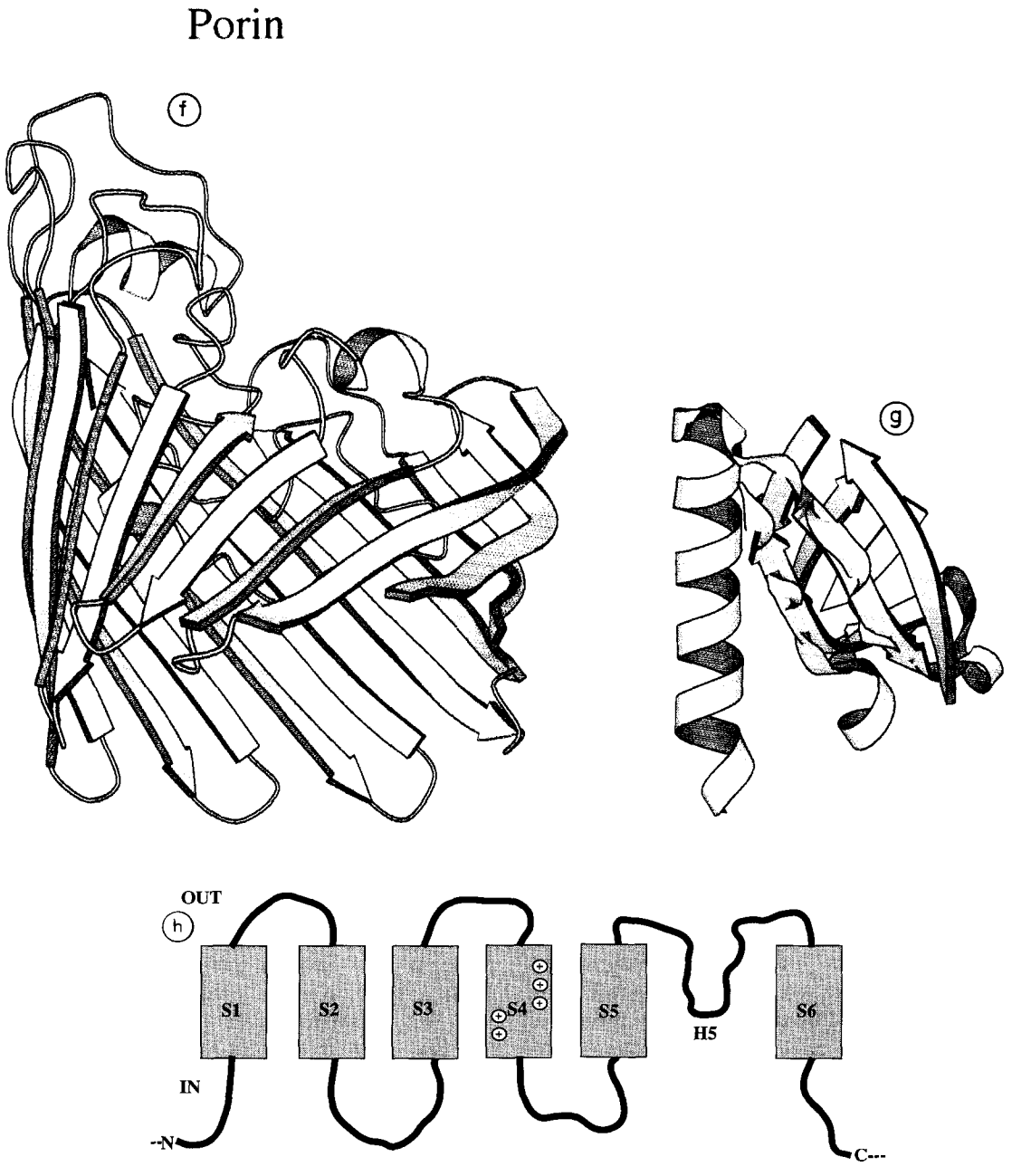

Fig. 1. Membrane protein topologies [14,193,224] (a) type I membrane protein (b) type II membrane protein (c) type III membrane protein. The former are bitopic membrane proteins. (d) a type IV or multi-spanning (polytopic) membrane protein; for examples of other polytopic proteins, see Figs. 1(h) and 4. The plus-signs refer to Lys and Arg side chains which are predominantly found inside the membrane (the positive inside rule [226]). (e) a monotopic membrane protein (prostaglandin H synthase, reprinted with permission from *Nature* [153]). The protein is dimeric; the four amphipathic helices which interact with the membrane are labeled A, B, C and D. (f) porin-type β-barrel: *Rb. capsulatus porin* [233] drawn using the program MOLSCRIPT by Kraulis [101]. (g) schematic model of an α/β membrane protein motif, proposed to be present in each of the five acetylcholine receptor subunits [218]. The fold shown is from cholera toxin β-subunit [195], drawn with MOLSCRIPT [101]. (h) tentative folding pattern of voltage-gated channels, which might comprise another type of α/β membrane protein; S1–S6 refer to the transmembrane segments which are thought to be helical; H5 refers to the pore region of the channel which might be in β-sheet configuration [154,252]. The plus-signs in S4 stand for the intramembranous Arg and Lys residues found in this segment; these are thought to comprise the voltage sensor of the channel.

typical transmembrane helix consists of about 20 consecutive non-charged amino acids that in an α-helical configuration can span the 30 Å long hydrophobic core of the lipid bilayer. As a 3_{10}-helix, a shorter peptide would also be capable of traversing the membrane. Furthermore, it has been argued [117] that in a multispanning membrane protein, such as the band 3 protein, helices which do not face lipids can be much shorter than 20 residues; in fact, according to Lodish [117], there is no reason why the interior of a large membrane protein should necessarily be helical at all. In the bacterial reaction center, the transmembrane α-helices are actually longer, ranging from 21 to 28 residues in length [127,128], but their non-charged region is only 25 Å or at least 16 amino acids long [55,128]. The non-charged region is covered by detergent in the crystals [171,172]. In bacteriorhodopsin the helix length varies between 20 and 27 residues. The helices are often longer than the canonical 20 residues either because they are tilted relative to the membrane plane, or because the helix ends are hydrophilic and extend for one or two turns to the aqueous phase. In the cases of plant light-harvesting complex and the aspartate chemoreceptor, much longer helices are observed due to long hydrophilic extensions of the actual transmembrane segments [105,189,214]. On the other hand, truncation experiments have shown that a 17 residues long transmembrane segment is needed for stable membrane insertion; however, a transmembrane segment as short as 12 residues was sufficient to render the model protein predominantly membrane-bound [42]. The study of Adams and Rose [2] yielded similar results.

Contrary to an α-helix under aqueous conditions, a transmembrane helix buried inside the lipid bilayer is a remarkably stable structure [53,244,249,250]. The main reason for this is the absence of water inside the bilayer and the lack of competition by H_2O for the hydrogen bonds that stabilize the α-helix. Consequently, a structure having a maximum number of hydrogen bonds satisfied intramolecularly such as an α-helix (or a β-barrel) is strongly favored over other configurations in the low dielectric environment. In addition to the highly favorable free energy of a hydrogen bond inside the bilayer, the hydrophobic effect (i.e., the hydrophobicity of the side chains) also makes a significant contribution to the membrane partitioning and stability of a transmembrane helix. The free energy of stabilization of a 20-residue transmembrane helix has been estimated to be on the order of 70 kcal/mol [53]. For comparison, the folded conformations of soluble proteins are stabilized by free energies ranging from 5–15 kcal/mol [138,160].

A transmembrane helix has often been thought to perform a rather passive function in most membrane proteins, being essentially a hydrophobic membrane anchor without much structural characteristics beyond non-polarity. However, recent studies suggest that membrane spanning segments do have some specific features [93,106,110, 150,194,227,249]. For example, intermolecular helix–helix

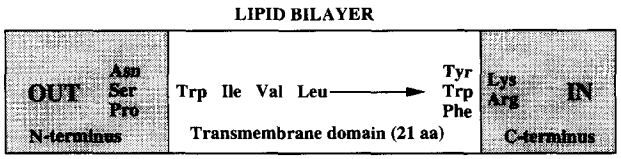

Fig. 2. Characteristic features of the single transmembrane segment of human type I membrane proteins according to Ref. [106]; see also [93]. In and out refer to the inside and outside of the membrane, respectively. Helix initiators Asn, Ser and Pro appear to be enriched in the N-terminal extracellular region preceding the transmembrane segment, whereas Lys and Arg residues are found in the intracellular part. Aromatic residues occur at interfacial positions. Residues which favor β-strand secondary structure are found in the C-terminal part of the transmembrane segment; the N-terminal half shows a preference for leucines (cf. [93]) which favor α-helical conformation. Ala, Gly and Phe were also found to be enriched in the transmembrane spans studied. For a more general sequence analysis of transmembrane segments, including those of multispanning proteins, see [93]. Adapted from Ref. [106].

interactions inside the lipid bilayer appear to be crucial for the function of many single-span membrane proteins (reviewed in [110,246]; see also [249]). In a number of homologous single-spanning membrane proteins, the transmembrane segments exhibit higher interspecies conservation than the soluble domains of the same proteins [202]. Landolt-Marticorena et al. [106] analysed the assumed transmembrane sequences and their flanking regions in 115 human proteins that have a single transmembrane span with N-terminus facing the outside, a topography classified as type I membrane proteins (Fig. 1). Clear trends were observed: six amino acids (Ile, Leu, Val, Ala, Phe, and Gly) appear to be enriched in the transmembrane segment. Of these, only Ala and Phe did not show any positional preference in the sequence. Leucine appears more often in the cytoplasmic half of the transmembrane segment while Ile and Val seem to prefer the cytoplasmic half of the helix. The suggested consensus sequence for human type I transmembrane segments is shown in Fig. 2. Trp, Tyr and Phe appear to favor an interfacial position, a feature that is also present in more complex membrane proteins (see below). In keeping with the positive inside rule of von Heijne et al. [6,194,223,224,226] which also applies to multispanning proteins, Lys and Arg residues were found to be enriched in the cytoplasmic sequence after the transmembrane segment. Glycine is found in transmembrane domains of multiple span proteins as well [93,227]. In general, helices in multispanning proteins appear to be more polar than those in single-span proteins [93].

A clustering of aromatic residues at the polar/non-polar interface is observed in the reaction centers, porins, prostaglandin H synthase and also in the peptide ionophore gramidicin A. In this latter case, the four boundary tryptophans may hydrogen-bond to the lipid headgroups or water and are likely to play a role in anchoring the peptide in a correct orientation within a bilayer [86]. The tryptophan dipole moments have their major component along the channel axis, which appears to be an important electro-

static factor controlling the cation channel function of gramicidin which has no charged residues [63,86,99]. Furthermore, studies with model compounds mimicking the side chain of a tryptophan show that an indole ring partitions spontaneously to the lipid headgroup region of a bilayer [236,240]. The driving force of this process has a substantial enthalpic component, implying that factors other than the hydrophobic effect (e.g., van der Waals interactions, hydrogen bonding) are also involved in stabilizing the interfacial location of tryptophans [240].

In proteins of known 3D structure the outer interface aromatic ring is more polar than the one at the inner interface, suggesting that this difference might be involved (in addition to the positive inside rule) in translocation and in orienting the protein within the bilayer [182]. Inspection of the reaction center structure shows that many tryptophans participate in hydrogen bonds with distant main chain carbonyls, which may contribute to the stability of the tertiary structure ([182]; see also [36]). Those tryptophans of the reaction center that reside in the hydrophobic core region appear to interact with the light-absorbing pigments ([128]; cf. [80]). In agreement, site-directed mutagenesis studies with bacteriorhodopsin and with another seven-helix protein of the rhodopsin family indicate that tryptophans in transmembrane segments, while not essential for function, participate in ligand binding [131,232] and also contribute to the stability of the protein [131].

Although proline is an α-helix breaker (see [38,46,239]), it is common in the transmembrane segments of type II and multispanning membrane proteins [17,93,225,227]. In particular, prolines are frequently found in the middle positions of transmembrane segments of multi-spanning proteins; these prolines tend to be highly conserved [93]. The presence of a proline in the middle of a helical segment often results in a kink and prevents the formation of several helical hydrogen bonds [239,225]. The proline causing the kink and the residues left without their backbone hydrogen bonds are usually on the open convex side of the helix [225]. Moreover, there appears to be a preference for polar side chains in the helical positions predicted to be on the convex side. In most cases, this side faces another helix or a cofactor and not the lipid ([225] but see also [9]).

Charged residues also occur in transmembrane segments, and they can in fact be stabilizing provided that they form ion pairs inside the bilayer [82,83]. The best characterized example is bacteriorhodopsin, in which several functionally important ion pairs are found [80,103,199]. Both structurally and functionally important charged residues occur in lactose permease [95,108,175]. Ion pairs appear to play a role in some interhelical interactions as exemplified by the structure of the light-harvesting complex [105], and they provide a mechanism for oligomerization of individual subunits (see below). Ion pairs may also be intrahelical, as is thought to be the case in the voltage sensor of voltage-gated potassium channels [51]; cf. [105].

3.3. β-Sheet structures

Unequivocal evidence for the presence of intrabilayer β-structures exists only in the case of porins; transmembrane β-sheets are also very likely to occur in the acetylcholine receptor [71,218,252]. As expected for a β-strand, 7–9 residues are needed to traverse the hydrophobic core of the membrane in porins [32,184,233]. Every second residue in the membrane spanning β-strand of porins faces the lipid and is thus hydrophobic. The rest of the residues can be either hydrophobic or hydrophilic depending on whether they are buried inside the protein structure or exposed to the porin channel. Hence, stretches of hydrophobic residues are not necessary to span the membrane. Strategies for sequence-based prediction of transmembrane β-strands are not as straightforward as those developed for transmembrane helices. For example the two *E. coli* porins and porins from phototrophic bacteria have similar 3D structures, even though they have non-related primary structures [104,183]. Yet, Schirmer and Cowan [184] have made use of the observations that every second residue in a porin transmembrane β-strand is hydrophobic and that aromatic residues cluster at the bilayer interface to predict the locations of the transmembrane β-strands in a porin. It is clear, however, that the development of accurate structure prediction algorithms requires a more extensive database than the one currently in existence. A major issue, for example, is the development of algorithms that accurately differentiate between a transmembrane α-helix and two or three consecutive membrane-spanning β-sheets [57,155,252].

3.4. Interactions between secondary structure elements

Analysis of bacterial reaction center structures [163] suggests that in a membrane spanning helix the amino acid residues facing the lipid moiety are more hydrophobic than those facing other helices, i.e., the transmembrane helices in multiple span proteins are often amphipathic. Moreover, the residues in contact with lipids are less well conserved than the residues which point toward the protein interior [93,163,164]. During evolution, lipid-facing residues have tended to become substituted with only certain residues. Consequently, analysis of substitution patterns in related sequences yields information on whether a helical surface is likely to be exposed to the lipid or buried in the protein interior [50,93] (although one should keep in mind that the predictive power of all the methods cited above has been verified with a very limited structural database). The packing density and hydrophobicity of the reaction center interior appears to be similar to that of water-soluble proteins [164], implying that van der Waals interactions are central for the interhelical interactions and stability of both types of protein [1]. Accordingly, the driving force for the

[1] The interiors of soluble proteins are tightly packed and are thought to be best approximated by crystalline small organic molecules [28,38,167].

helix–helix association inside the bilayer is thought to be mainly enthalpic [54,231,243], although the 'lipophobic' nature of membrane proteins may also be caused in part by the entropic preference of a lipid molecule to maintain as many lipid neighbors as possible [54].

The interaction between two helix macrodipoles would be expected to favor antiparallel association of two neighboring helices. In practice, both antiparallel (e.g., the bacterial reaction centers, bacteriorhodopsin and rhodopsin) and parallel (plant light-harvesting complex, glycophorin A dimer, bacterial chemoreceptor dimers) arrangements are observed. In fact, the energy gain due to the antiparallel alignment of the helices has been estimated to be quite small, on the order of 1–2 kcal/mol in the *Rhodobacter sphaeroides* reaction center [26]. Theoretical work suggests that the strength of the interaction between helix macrodipoles depends on the degree of the exposure of the helix ends to water [70].

As mentioned above, charged residues, although not common, do occur in transmembrane segments. The recently published structure of plant light-harvesting complex shows that two interhelical Glu-Arg ion pairs are present [105]. The function of bacteriorhodopsin depends on intramembrane acidic and basic residues [80,103]. Several salt bridges with distinct functions have been identified in the transmembrane segments of lactose permease [95]. Furthermore, charged residues in the single transmembrane domains of certain T-cell receptor subunits appear to play an essential role in the assembly of the receptor complex [30,124,174].

In the majority of helix–helix interactions, charged residues are not required [253]. For example, glycine-rich sequences mediate the association of α- and β-chains of the class II major histocompatibility complex [29]. (In this process, an ion pair as well as complementary packing interactions play only facilitative roles causing heterodimers to be favored over homodimers [29].) A recent cysteine mutagenesis and disulfide cross-linking study suggests that the contact surface between the two transmembrane helices of the *E. coli* leader peptidase is composed of non-charged residues [237]. Similarly, the dimerization of the red cell sialoglycoprotein glycophorin A (a type I membrane protein; see Fig. 1) occurs solely through its transmembrane segment that does not have any charged residues [15,65,111]; cf. [249]. Glycophorin A dimer is stable in the presence of SDS, enabling direct detection of the dimers using SDS-polyacrylamide gel electrophoresis. Furthermore, a chimera of the normally monomeric soluble enzyme staphylococcal nuclease and the transmembrane domain of glycophorin A also forms SDS-stable dimers and can be purified with methods worked out with the nuclease [111,112]. Dimerization of the chimera can be specifically and competitively inhibited with peptides having the same sequence as glycophorin A transmembrane domain. Mutational analysis of the transmembrane domain of the chimera [112] shows that the dimerization is in part controlled by a five-residue sequence motif found also in the single transmembrane segments of a family of growth factor receptors, such as the neu receptor [22,203,204] and other transmembrane proteins [130,249] which also exist as dimers. It is noteworthy that a point mutation within the sequence motif in the neu receptor results in malignant growth, probably due to the formation of permanent rather than transient, ligand-induced dimers [203] (see Fig. 3a). Yet it is unclear how the Val → Glu mutation in position 3 of the Sternberg–Gullick motif [203] could bring about dimerization since according to the analysis of Lemmon et al. [112] this residue should not reside at the dimer interface.

The proposed oligomerization motif comprises five consecutive residues: The first position is occupied by a small residue (Gly, Ala, Ser, Thr, or Pro), the fourth by an aliphatic one (Ala, Val, Leu, or Ile) and the fifth residue is either Ala or Gly [203,204] (Fig. 3a). In glycophorin A the first as well as the last residue of the motif is glycine. All tested substitutions of either Gly abolished dimerization completely (with the exception of replacing the first Gly by Ala, which resulted in only partial loss of dimerization) [112]. However, in glycophorin A several critical residues fall outside of the five residue motif (Fig. 3b). In particular, one Thr and two aliphatic residues that in an helical projection reside on the same face with the essential glycines perform a role in dimer formation; it seems that the interhelical surface covers about two-thirds of the length of the glycophorin A transmembrane segment [112] (see Fig. 3b). It has in fact been proposed that the actual

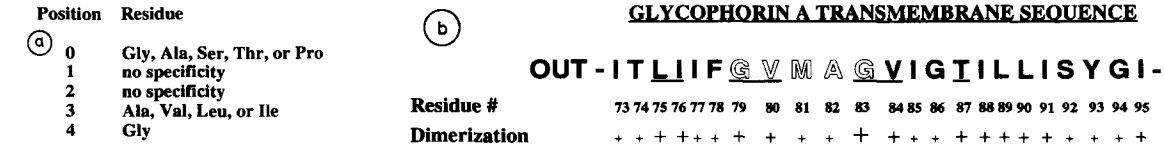

Fig. 3. (a) The five-residue oligomerization motif in transmembrane helices [203]. In the oncogenic form of the neu receptor (a tyrosine kinase linked growth factor receptor), the P3 Val residue of the wild-type receptor has been replaced by a Olu, resulting in constitutive activation of the receptor and transformation of the affected cells. (b) Analysis of residues involved in the formation of a glycophorin A dimer (adapted from [112]). The larger the + symbol, the more important is the residue for dimerization. Residues involved in glycophorin A dimerization were identified using site-directed mutagenesis and SDS-PAGE [112]. The average effect of several substitutions of each residue along the transmembrane helix by non-polar residues is shown. The five-residue motif of Sternberg and Gullick [204] is outlined; amino acids that comprise the seven residue dimerization sequence LIxxGVxxGVxxT [113] are underlined. In an α-helix, these residues are on the same side of the helix. For related studies with another model protein, see [249].

dimerization motif reads LIxxGVxxGVxxT, which, when placed into a polyleucine peptide, causes specific dimerization of the peptides [113]. Further, a Fourier transform analysis of the contribution of each residue along the transmembrane segment to the dimer disruption indicates a period of 3.9 Å (instead of the standard value of 3.6 Å for a regular α-helix), suggesting that the two interacting helices form a right-handed supercoil [112]. In agreement, a molecular modeling study using simulated annealing indicates that the two helices could form a right-handed coiled coil with the helical axes approaching as close as to within 7 Å of each other at the first essential glycine and with an interhelical hydrogen bond between the essential threonines [216] (see Fig. 3b). For analogous mutagenesis and modelling studies with phage M13 coat protein, see Ref. [249].

In the porin trimer, the β-barrel of each monomer interacts with its two neighbor monomers, resulting in a very rigid interaction surface with low crystallographic temperature factors [233]. The proportion of the residues involved in the subunit–subunit contacts varies between 23 and 28% among different porins [32,104,233]. The intersubunit interactions are mediated by a number of hydrogen bonds located mostly at the level of outer surface of the bilayer and in the outer loops, and by van der Waals forces among several phenylalanines situated at the level of the hydrophobic core of the bilayer. The N- and C-termini of each monomer form ion pairs at the interface thereby rigidifying the structure further [32,104,233]. In the *E. coli* porins [32], phenylalanines appear to interact with small residues in neighboring β-barrel. An additional stabilizer in the *Rb. capsulatus* protein are three calcium ions which are chelated between each monomer [31,188,233].

4. Thermal stability of membrane proteins. Survey of experimental results

Contrary to the case of water soluble proteins, only a few membrane proteins have been thoroughly studied by high sensitivity differential scanning calorimetry (DSC) (which is the method of choice if quantitative thermody-

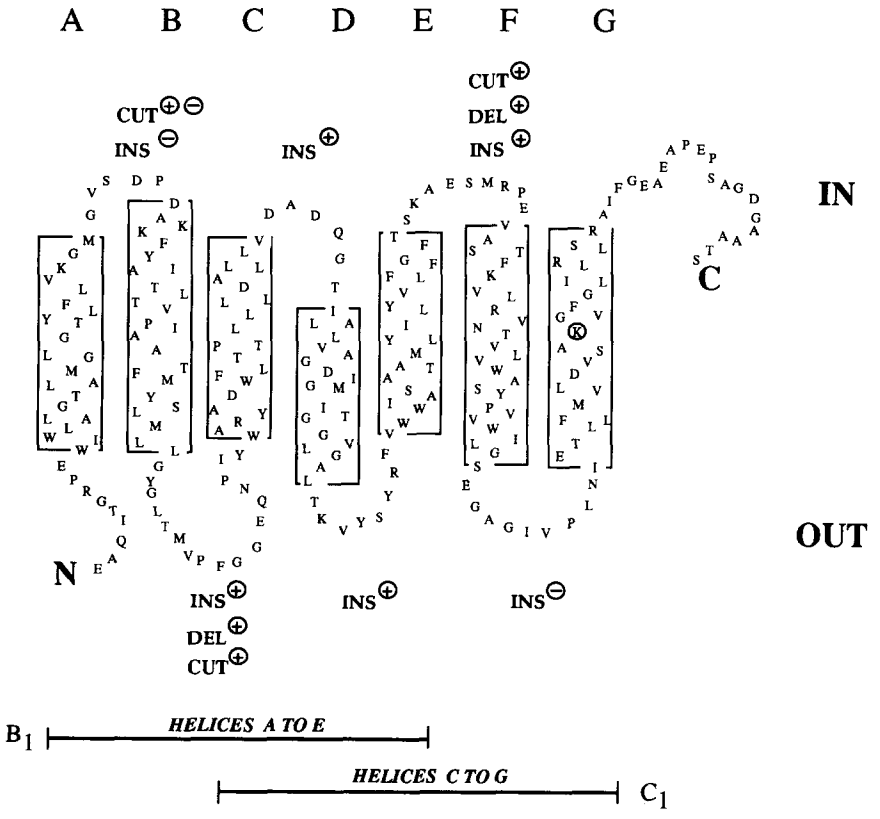

Fig. 4. Bacteriorhodopsin membrane topology. The seven transmembrane helices, designated A to G, are shown. Retinal binds to Lys-216 in helix G (encircled). 66 % of the residues are located in the transmembrane domains. Cut^+ = continuous backbone in this loop is not necessary for folding to a native-like structure; Ins^+ = this loop tolerates an insertion; Del^+ = this loop can be shortened and the protein is still functional. Minus-superscript in the previous characters denotes the opposite effect. In loop A/B, a covalent link was found necessary for functional reconstitution by Liao et al. [116]; in the peptide work of Kahn and Engelman [96] no continuous backbone in the loop was required for folding, but the peptides used to form helices A and B overlapped in the loop region. The bars marked B1 and C1 refer to the fragments composed of helices A–E and C–G, respectively. Despite both of the fragments contain transmembrane helices C, D and E, they can be combined to make functional bacteriorhodopsin [116]. Thus the overlapping segments do not interfere with folding (while neither fragment alone is functional). For other references, see the text.

namic information is to be obtained). Moreover, the stability of a membrane protein with a large surface area exposed to the bilayer is expected to be a function of the amphiphile used to disperse the protein. In most cases the role of the amphiphile has not been systematically studied. Below, we summarize the results available.

4.1. Bacteriorhodopsin

Bacteriorhodopsin (M_r = 26 kDa) is a light-driven proton pump that converts solar energy into a proton electrochemical potential. It is the sole protein component of the purple membrane of archaebacterium *Halobacterium salinarium* (formerly *H. halobium*); the purple membrane is, in fact, a 2D crystalline array of hexagonally organized bacteriorhodopsin trimers (see Figs. 4–6). Monomeric bacteriorhodopsin is, however, also functional. The stability of bacteriorhodopsin has been studied calorimetrically both when in the purple membrane [20,90,191] and also when in the monomeric state in detergent-lipid micelles [21].

By weight, 75% of the purple membrane is bacteriorhodopsin and there are only about 10 lipid molecules per bacteriorhodopsin molecule in the membrane [98]. A large fraction of the lipids are unusually polar owing to the presence of sulfate headgroups. Although a minor component of the membrane, the lipids play a specific role in the 2D crystal lattice of bacteriorhodopsin molecules [158,200,201], probably because the charged polar headgroups are involved in lattice formation. The crystal lattice is composed of bacteriorhodopsin trimers which are further organized to form hexagonal crystals (Fig. 6). It is precisely those crystals of the native purple membrane that were used in the determination of the current structural model of bacteriorhodopsin [80]; see Fig. 5.

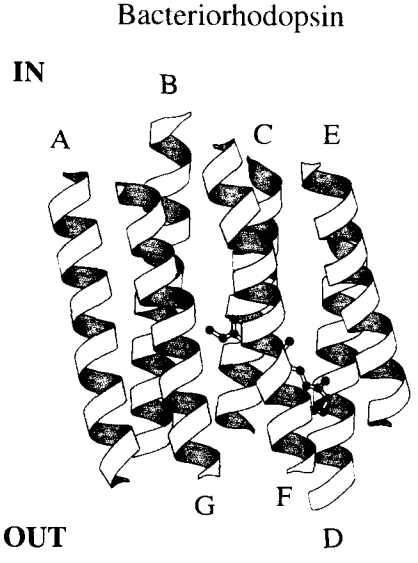

Fig. 5. The transmembrane helices of bacteriorhodopsin seen from the membrane plane. Retinal bound the Lys-216 of helix G is shown as ball and sticks model. The structure of the extramembrane loops is not shown. The letters A–G refer to the helices shown in detail in Fig. 4. The figure was drawn with the program MOLSCRIPT [101] using the coordinates of Henderson et al. [80].

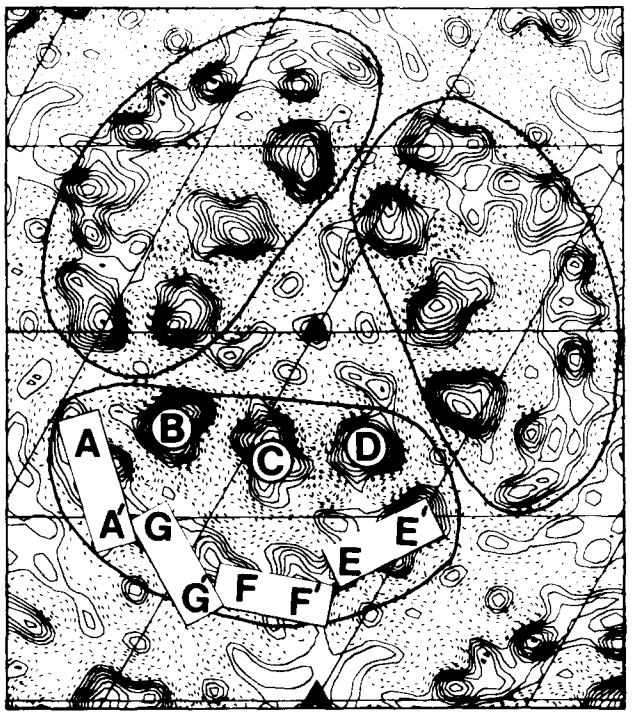

Fig. 6. Electron density map of the purple membrane of *Halobacterium salinarium* (reproduced with permission from Ref. [207]) showing a bacteriorhodopsin trimer. Helices A, G, F and E are tilted relative to the membrane normal, and their extracellular ends are marked with A′, G′, F′ and E′, respectively. Note that the intermonomeric contact occurs mainly between helices B and D, and, to a lesser extent, between helices A and E.

A prominent feature of the bacteriorhodopsin structure is a bundle of seven transmembrane helices connected by short extramembrane loops and possibly two or three short helices parallel to the membrane plane (Fig. 5). All the transmembrane helices contribute to the binding site of the prosthetic group, retinal [73,80]. Upon absorbing a photon, the chromophore isomerizes from an all-*trans* to a 13-*cis* form, which then leads to proton translocation assisted by movements of the transmembrane helices [173,207]. A recent analysis [166] based on the cryo-electronmicroscopic structural model of Henderson et al. [80] suggests that the external surface of bacteriorhodopsin is relatively hydrophilic in contrast to the original prediction [163] but consistent with the recent theoretical work of Donnelly et al. [50]. Considering the structure of the purple membrane, it is possible that some of the exposed polar residues may actually not face lipids. Instead, they may face other bacteriorhodopsin molecules and participate in the formation of the 2D lattice. In the bacteriorhodopsin trimer, the intermonomer contacts occur primarily between helices B and D and to a lesser extent between A and E (cf. [207]), all of which contain some polar residues (see Figs. 4 and

6). In particular, helix D has a Gly-rich external face that appears to interact with helix B [50,80,166,207].

From the above discussion it is evident that the structural stabilization of bacteriorhodopsin must involve intramolecular interactions, intermolecular interactions, interactions of the protein with the lipid bilayer and also interactions with the retinal chromophore.

The calorimetric scans of bacteriorhodopsin in the purple membrane are complex, exhibiting several reversible pretransitions in addition to the major, irreversible transition with a T_m near 100°C at neutral pH [20,90,191]. The major, irreversible transition corresponds to the denaturation of the protein and has a calorimetric enthalpy of approx. 100 kcal/mol (3.7 cal/g) at 100°C and neutral pH. This value is substantially smaller than that of a typical soluble protein at the same temperature (12 cal/g). One of the pretransitions below 80°C coincides with a 100 nm blue-shift in the optical spectrum of the bound retinal [20,90].

Monomeric micellar bacteriorhodopsin is less stable than the trimeric bacteriorhodopsin in the purple membrane [21]. The main denaturation transition of this species is centered at 80°C. Remarkably, the measured enthalpy change for both species is similar ($\approx$ 100 kcal/mol), suggesting that the major stabilizing effect of the crystal lattice is of an entropic origin and that the entropy term contributes about 5 kcal/mol to the free energy of stabilization. The monomeric protein also exhibits a calorimetric pretransition detectable as a 100 nm blue-shift in the visible spectrum of the chromophore [21]. Presumably, this pretransitional rearrangement within a monomer acts as a trigger for further rearrangements within the crystal lattice [20,90,191].

According to Jackson and Sturtevant [90] and Brouillette et al. [20] the calorimetric scans of bacteriorhodopsin do not depend on the scanning rate suggesting that the processes observed reach equilibrium during the measurement and that the irreversible step occurs at a later stage. However, these results differ from those of Galisteo and Sanchez-Ruiz [66] who found a significant scanning rate dependence.

For the trimeric protein, the ratio of $\Delta H_{vH}/\Delta H_{cal}$ is clearly higher than 1 and approaches the value of 3, suggesting intermolecular cooperativity and that in the purple membrane the protein most likely denatures as a trimer [20,90,97]. Consistent with this interpretation, $\Delta H_{vH}/\Delta H_{cal}$ for monomeric bacteriorhodopsin is close to 1 [21]. (However, according to the analysis of Galisteo and Sanchez-Ruiz [66] and Morin et al. [134], the ratio of the van 't Hoff enthalpy to the calorimetric enthalpy cannot be used by itself as a measure of the cooperativity of the transition, if the transition is scanning-rate dependent.) As discussed above, interactions within the crystal lattice contribute about 5 kcal/mol to the free energy of stabilization, increasing the transition temperature from about 80 to 100°C. The disruption of the interactions within the lattice triggered by the denaturation of the first protein molecule will immediately lower the transition temperature of the remaining two molecules in the trimer. Since this process occurs at 100°C, the remaining molecules will immediately find themselves above their transition temperature resulting in a cooperative denaturation cascade.

A direct determination of ΔC_p from a thermogram of bacteriorhodopsin has not been possible; however, Brouillette et al. [20] have shown that above 80°C the enthalpy change increases linearly with temperature with a slope of 0.046 cal $K^{-1}g^{-1}$. This is a remarkably low value (about 3 times smaller than the ΔC_p of myoglobin for example), especially considering that bacteriorhodopsin is an integral membrane protein with a large fraction of hydrophobic residues.

The extremely low ΔC_p suggests that upon denaturation not a very large number of hydrophobic groups become exposed to water. This observation is substantiated by the additional result that the calorimetric enthalpy of monomeric bacteriorhodopsin exhibits no clear temperature dependence when the protein is reconstituted using a large excess of lipids and detergent [21]. Under these conditions, a larger fraction of hydrophobic residues may not become exposed to water but to lipid upon denaturation, resulting in an even smaller heat capacity change.

Another important conclusion from the calorimetric experiments is that the enthalpy change is smaller than the change expected for the complete unfolding of a water soluble protein of similar molecular weight. It should be noted that the unfolding enthalpy of a transmembrane helix must be significantly higher when the unfolding is not accompanied by exposure to water, since the disruption of intramolecular hydrogen bonds will not be compensated by the formation of hydrogen bonds with water. The small experimental enthalpy suggests that the transmembrane helices do not unfold upon thermal denaturation. This conclusion agrees with the observation that the main calorimetric transition is not accompanied by a major change in the CD spectrum of the protein. The relatively minor temperature-dependent changes seen in the CD spectra might be accounted for by the unfolding of the hydrophilic ends of the transmembrane helices and by the unfolding of the putative helices that run parallel to the membrane plane (cf. [80]).

Denatured, retinal-free bacteriorhodopsin refolds in vitro in the presence of lipids and/or detergent [16,87,115,158]. The refolding process takes place in two main steps which occur in the time scale of minutes. In the first step, the individual helices form and associate and, in the second, added retinal binds stoichiometrically to the apoprotein, regenerating the native chromophore. Renatured monomeric bacteriorhodopsin pumps protons and can be reconstituted with *H. salinarium* lipids to form the crystal lattice characteristic of the purple membrane. Similar results have been obtained by using two denatured chymotryptic fragments (corresponding to helices A and B,

and C to G) as starting material [87,115,158]. A covalent link between helices A and B is also not critical for bacteriorhodopsin structure (but see [116,211]), as the AB fragment can be substituted by two synthetic peptides, corresponding to the individual helices A and B, in the above experiment [96]. Analogously, fragments composed of helices A-to-E and FG assemble in the presence of retinal to produce a native-like bacteriorhodopsin lattice, showing that a continuous loop between helices E and F is not structurally essential either [116,192]; cf. [54]. Functional bacteriorhodopsin has been reconstituted from two overlapping fragments that have three helices in common; thus the redundant helices appear not to interfere with the assembly process [116]. By contrast, the folding process appears to be sensitive to lengthening of the short loops between helices A–B and F–G [211], suggesting that the structure of the loops affects helix–helix packing.

In a recent molecular simulation study [217], it was found that (i) the positions of the seven helices could be predicted rather accurately by conformational energy optimization without considering the extramembrane loops; that (ii) retinal appears to affect the positions of helices D, E and F much more than that of the other helices; that (iii) the bent helix C (which has a proline residue exposed to lipid [225]) has a central role in the energetics of bacteriorhodopsin while helix D appears least important in this respect; and that (iv) helices A and B are relatively independent of the rest of the molecule (see Fig. 5).

Although helix–helix interactions appear to be the decisive factor in bacteriorhodopsin folding, recent calorimetric work shows that the extramembrane loops do contribute to the stability of bacteriorhodopsin structure, both enthalpically and entropically [97]; cf. [69]. For instance, a cut between helices B and C in bacteriorhodopsin embedded in the purple membrane decreased the T_m by 6°C and diminished the enthalpy change from 100 kcal/mol to 56 kcal/mol. In vesicular bacteriorhodopsin, the same cut decreased T_m by 12°C and the enthalpy by 33 kcal/mol, whereas the loss of the covalent bond between helices A and B caused a further 12°C and 47 kcal/mol drop in the T_m and enthalpy, respectively. Removal of retinal destabilized the protein approximately as much as the loss of two covalent connections in the extramembrane loops [97]. Despite the reduced stability and the loss of covalent bonds, only one peak with $\Delta H_{vH}/\Delta H_{cal} > 1$ is observed in DSC, suggesting that both intra- and intermolecular cooperativity are still preserved [97]. These studies also suggest that a large part of the enthalpy change for denaturation either is directly contributed by the extramembrane loops or results from the disruption of helix–helix interactions, the strength of which is regulated by the loops.

About 90 out of the 248 residues in bacteriorhodopsin are located in the extramembrane loops, corresponding to a molecular mass of 9500 Da. Assuming that the loops behave as in small soluble proteins, one can calculate that their unfolding should give rise to an enthalpy change of about 114 ± 11 kcal/mol at 100°C. This value reasonably close to the observed enthalpy change (100 kcal/mol; [20]) measured for the thermal denaturation of whole bacteriorhodopsin. However, the study of Kahn et al. [97]

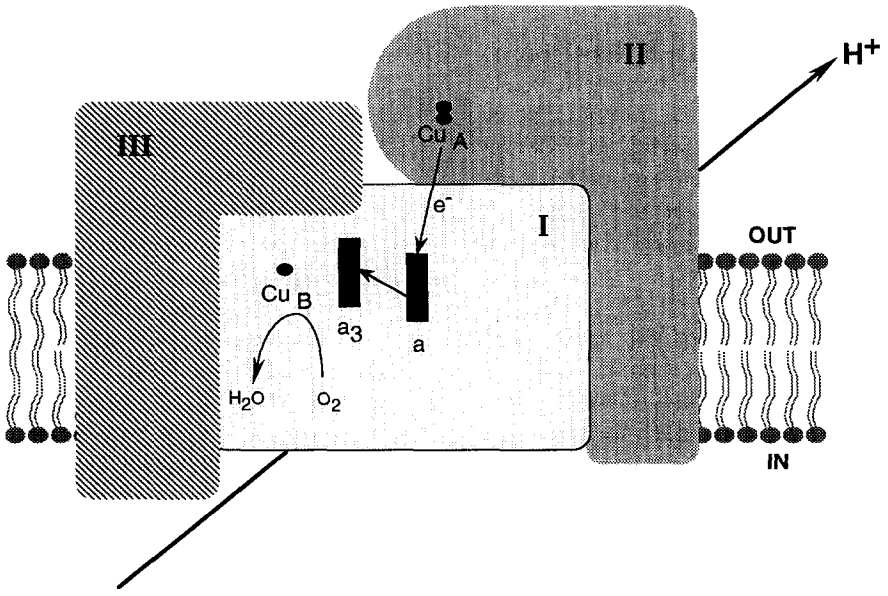

Fig. 7. A schematic model of the major subunits (I, II and III) of cytochrome-*c* oxidase. The electrons from cytochrome *c* center at a binuclear copper center, Cu_A, in subunit II. From this center they go to the low spin heme (heme *a*) and then to the iron-copper oxygen reducing center formed by heme a_3 and Cu_B. The latter three metal sites are located in subunit I, which is thought to contain 12 transmembrane segments. Electron transfer from cytochrome *c* to oxygen is coupled to proton translocation across the membrane. Subunit III comprises a separate domain which interacts weakly with the rest of the enzyme; it does not contain any prosthetic groups. In accord with the results in [77], subunit III is depicted as having both a transmembrane and a peripheral domain.

suggests that a large part of this enthalpy (77%) is contributed by binding of retinal, the binding site for which is located in the center of the protein away from the loop region [80]. Of course, it is not impossible that the loops are largely unfolded in the absence of retinal. A similar calculation using the average heat capacity change of soluble proteins yields a ΔC_p of about 1240 cal mol^{-1} K^{-1} for the loop region only, whereas the measured value is about 1200 cal mol^{-1} K^{-1} [20]. One can conclude that the calculated values appear to agree strikingly well with the idea that only the extramembrane parts unfold and become exposed to water upon denaturation.

4.2. Cytochrome-c oxidase

Cytochrome-*c* oxidase is a multisubunit membrane protein found in eukaryotes, eubacteria and archaea (for reviews see [24,74,84,122,179]. It functions as the terminal oxidase of the respiratory chain, oxidizing ferrocytochrome *c* and reducing dioxygen to form water. Part of the energy available in this redox reaction is used to translocate protons across the membrane housing the oxidase.

Although long thought to be present only in mitochondria and in the cytoplasmic membranes of only a few aerobic bacteria, it has recently become clear that cytochrome-*c* oxidase in fact belongs to a large superfamily of related enzymes with a wide occurrence on Earth. Some members of the family oxidize quinols instead of cytochrome *c*; there are also examples of alternative cytochrome-*c* oxidases [67,72,159] that are only distantly related to the enzyme discussed here. Most recently, a homology to a denitrification enzyme has been found, perhaps pointing to the ancient origin of the oxidase [24,180,221]. Homologous cytochrome oxidases from thermophilic [89,126], thermoacidophilic [118] as well as alkalophilic [162] organisms have been reported, showing that the same basic theme can be utilized in a wide variety of environments.

The subunit composition of cytochrome-*c* oxidase depends on the source of the enzyme: In mitochondria, the enzyme comprises 13 dissimilar polypeptides, resulting in a molecular mass of 205 kDa, whereas the bacterial oxidases have typically three or four subunits and a molecular mass of about 130 kDa (see Fig. 7). But regardless of the organism, the catalytic metal centers (two heme irons and two copper sites) are located in a core made up by subunits I and II. The complex of these two subunits is sufficient for redox-linked proton translocation in vitro [76,81,206], although the presence of a third subunit improves the energy transduction efficiency [205]. Subunit III may influence the oxygen reduction site [77]. Yet, the exact function of the third subunit as well as that of the other subunits with no redox-active metal sites remains obscure. In a recent study, using a homologous quinol oxidase, it was shown that the three largest subunits can be fused without adverse effects on folding or activity [120].

Hydropathy analysis, biochemical and gene fusion experiments suggest that subunits I and III are mostly helical, whereas subunit II has only two N-terminal transmembrane helices; its C-terminal part is thought to make up an extramembrane domain with a high β-sheet content and the cytochrome-*c* binding site [27,107,179]. A large extramembrane domain has also been visualized in electron-microscopic work (reviewed in Ref. [257]) which suggests that about 50% of the oxidase resides outside the membrane on the cytoplasmic side of the mitochondrial membrane [43]. According to the same work, the intramembrane part of the protein consists of two domains [43], but these could not be seen in the electron crystallographic model of Valpuesta et al. [219]. However, according to the recent analysis of Frey and Murray [64], there might be three membrane-buried domains (designated M1, M2 and X) and one membrane-exposed domain (C) in the bovine enzyme crystallized as monomers using the detergent deoxycholate. When the structures of two monomers are superimposed, the structure of the resulting computational dimer closely fits the image of the oxidase crystallized in the dimeric form [64].

CD spectra indicate that 40% of the bovine heart oxidase has an α-helical secondary structure [149], in agreement with Fourier transform IR (FTIR) work of Arrondo et al. [8]; another FTIR study suggests α-helicity of 60% [25]. A low-resolution electron crystallographic structure of dimeric, lipid-embedded cytochrome-*c* oxidase is, however, consistent with only 12–16 transmembrane helices [219]. While this estimate is in line with the α-helix content of 40% based on the above CD and FTIR measurements, one should note that hydropathy analysis predicts 21 transmembrane helices in subunits I, II and III alone (see [23,179]). Unless the extramembranous portions of the oxidase molecule are completely devoid of α-helices, the hydropathy analysis probably overestimates the number of transmembrane helices.

Thermal denaturation does not cause a significant change in the amount of α-helix in beef cytochrome-*c* oxidase [8], suggesting that the transmembrane helices of the oxidase do not unfold thermally in a lipid environment. Likewise, in a detergent solubilized bacterial oxidase two thirds of the helices are preserved even at 77°C [77]. In the guanidine hydrochloride denaturation studies of Hill et al. [85], the helicity of beef oxidase exhibits a biphasic dependence on the denaturant concentration. About 70% of the far-UV CD signal at 222 nm remains at 1 M denaturant and is highly resistant against further increases in the denaturant concentration [85]. The first, denaturant sensitive phase was assigned to the extramembrane part of the complex.

To date, cytochrome-*c* oxidase from bovine, yeast and the bacterium *Paracoccus denitrificans* has been studied by DSC [77,133,134,168,169,190,245].

The early studies with the beef oxidase addressed mainly the lipid–protein interaction [168,190,245]. In the presence

of endogeneous lipids that remain associated to the oxidase after cholate-ammonium sulfate fractionation, the cholate solubilized enzyme was shown to denature at 63–64°C [245]. Delipidation shifts the T_m downwards by approximately 5°C; the enthalpy of denaturation was found to be highly variable depending on the lipid species used in subsequent reconstitution experiments [245]. Some of the effects observed by Yu et al. [245] could be speculated to be caused by liquid-to-gel lipid phase transition linked to protein denaturation (see Sections 4.3 and 7.1). Calorimetric work by Semin et al. [190] and Rigell et al. [168] shows that one oxidase molecule perturbs the thermotropic properties of 70–100 lipid molecules (corresponding to 0.25–0.35 mg lipid/mg oxidase), a number that corresponds roughly to the number of lipid molecules that can be fit in one layer around the oxidase molecule. There is a preference for cardiolipin in the lipid annulus surrounding the enzyme in the membrane [190], which has also been verified by other methods (reviewed by Robinson [170]).

Rigell et al. [168] using beef oxidase reconstituted with dimyristoyl phosphatidylcholine showed that the oxidase thermogram is in fact composed of two peaks centered at 52°C and at 64°C, respectively. The low temperature peak corresponds to the melting of subunit III, which although irreversible, is relatively close to a two-state process ($\Delta H_{vH}/\Delta H_{cal} = 0.85$; cf. [77]). The enthalpy of subunit III transition is 4.8 cal/g. The rest of the enzyme denatures in a multiphasic process with at least three sequential melting steps above 60°C [168,169]. When the oxidase is solubilized with the detergent Tween 80, the heat capacity function displays only one broad peak at 56°C, i.e., the high temperature transition appears to be sensitive to the detergent used and shifts to a lower temperature. The enthalpy of denaturation for the lipid reconstituted and detergent dispersed enzyme are similar and close to 500–600 kcal/mol (2.7 cal/g) [168]; a value much lower than the one expected for a water soluble protein at the same temperature (6.9 ± 0.8 cal/g).

A lipid reconstituted preparation of yeast cytochrome oxidase melts with an enthalpy of about 425 kcal/mol (2.4 cal/g assuming a molecular mass of 175 kDa for the preparation used) [134]. At low ionic strength, low and high temperature transitions similar to those described above with the beef enzyme are observed; at high ionic strength, the transition profile is less well resolved owing to a downward shift of the high temperature transition [133]. Three transition components, corresponding to the melting of subunits I and II, subunit III and subunits IV and VI, could be identified by a thermal gel analysis that makes use of the change in solubility of the subunits upon denaturation [134,169]. As in the case of the beef enzyme, subunit III also exhibits the lowest transition temperature. The midpoints of the transitions are scanning rate dependent, indicating that the denaturation process is kinetically controlled and characterized by an activation enthalpy on the order of 40 kcal/mol [134].

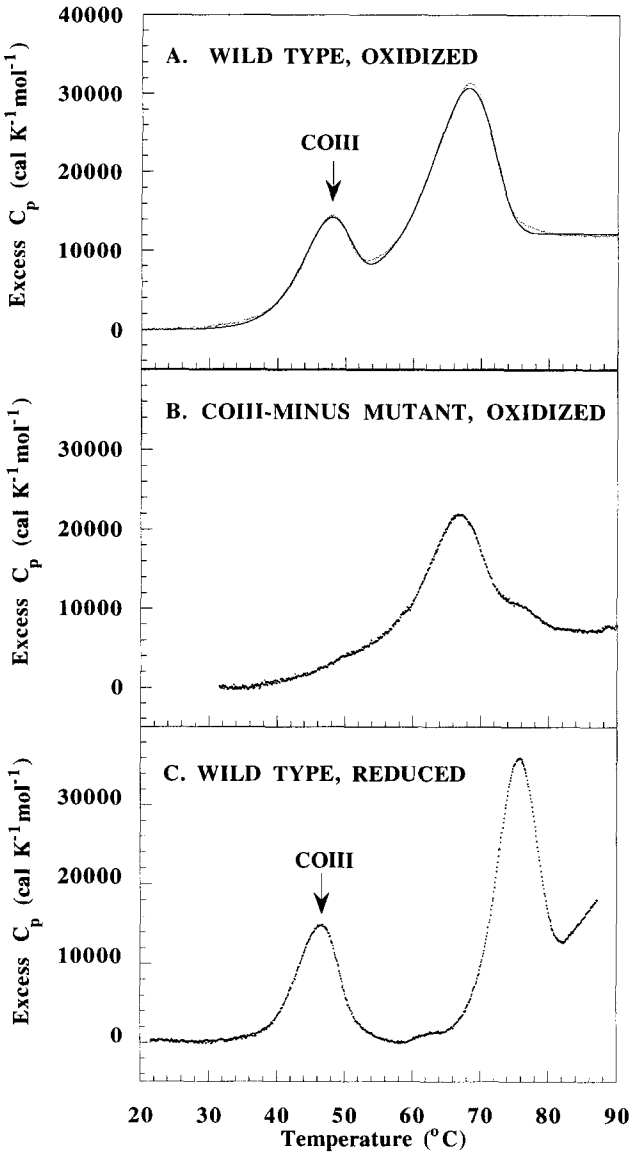

Fig. 8. DSC scans of cytochrome c oxidase from *Paracoccus denitrificans* [77]. Upper panel, oxidized wild type enzyme. The solid line is a theoretical curve calculated using a multistate kinetic model [134]. Both the low and high temperature peaks can be modeled as irreversible two-state transitions. Middle panel, oxidized enzyme purified from a mutant strain lacking the gene for subunit III. Lower panel, wild-type oxidase scanned while reduced with dithionite. COIII, subunit III.

The separation of the thermogram into low and high temperature peaks is clearest with the cytochrome $-c$ oxidase from *Paracoccus denitrificans* (see Fig. 8) [77]. This enzyme has only three (or four) subunits, simplifying the interpretation of the thermogram. In the dodecyl maltoside solubilized enzyme, subunit III is clearly the least stable part of the complex with a near two-state transition (ΔH_{cal} = 90–100 kcal/mol) at 46–48°C. The complex of subunits I and II denatures at 66–68°C in the oxidized enzyme; the transition can be modeled as an irreversible two-state transition [77] using the formalism described by Morin et al. [134]. In the reduced enzyme, the latter

transition not only shifts to a higher temperature (T_m = 76°C) but also becomes much sharper (Fig. 8). The high temperature transition in the reduced enzyme can also be modeled as a two-state transition. More complex explanations, such as a redox-state dependent interaction between subunits I and II, for the sharpening effect are possible, however. At any rate, these two subunits interact strongly defining one structural unit from which subunit III is clearly separate. Consistent with this idea, a two-subunit enzyme preparation, purified from a mutant that lacks the gene for subunit III [75] yields a thermogram with a single peak centered at 66°C. This result also suggests that subunits I and II are able to fold correctly (or at least very nearly so) in the total absence of the third subunit. The folding must be a multistep process in which the formation of the oxidase core, made up by subunits I and II, precedes a later step in which subunit III associates to the core (see [75]). The total calorimetric enthalpy changes for the wild-type and subunit III-minus enzymes are 350–380 kcal/mol (2.9 cal/g) and 250 kcal/mol (2.8 cal/g), respectively [77].

The thermal denaturation of the detergent solubilized bacterial oxidase has been measured with the most sensitive instrumentation available, under circumstances in which no precipitation effects interfere with the transition. Under those conditions a ΔC_p of approx. 12 kcal $mol^{-1}K^{-1}$ (~ 0.095 cal $K^{-1}g^{-1}$) was observed directly in the calorimetric thermogram. This result implies that upon thermal denaturation, a significant number of hydrophobic groups become exposed to water under the conditions used in those experiments (0.03% (w/v) detergent concentration in the buffer). It must be noted, however, that the observed ΔC_p is lower than the one expected for a highly hydrophobic protein (e.g., the ΔC_p associated with the thermal unfolding of myoglobin is 0.15 cal $K^{-1}g^{-1}$).

As in the case of bacteriorhodopsin, the enthalpy changes for the thermal denaturation of the oxidases from beef, yeast and bacterial sources are very similar when normalized on a weight basis (2.7, 2.4 and 2.9 cal/g). In all cases the enthalpy change is lower than the entire range of values found for water soluble proteins, reflecting the highly thermostable nature of the transmembrane segments of the enzyme. However, extrapolation of the enthalpy change for subunit III of the bacterial enzyme to the transition temperature of the two other subunits, using the measured ΔC_p of the low temperature transition, yields a ΔH of 5.5–6.5 cal/g for subunit III, which is significantly higher than the value for the two catalytic subunits. As the average enthalpy value for soluble proteins at 67°C is 7.8 ± 0.7 cal/g [138], it appears that subunit III has an enthalpy value intermediate between that of a typical membrane and a soluble protein. One possible explanation of this result is that subunit III is more exposed to the aqueous phase than is currently thought (cf. [179]), its unfolding and subsequent hydration being therefore more complete than that of the two other subunits (see [77]). It should be noted that at least one hydropathicity-based sequence analysis method predicts only four (and not seven) transmembrane helices in subunit III [44]. A number of results, including those cited above, are consistent with the view that subunit III makes up a largely independent domain. Considering the novel structural model of Frey and Murray [64], it is tempting to suggest that subunit III comprises the X domain of the model. In any case, two obvious but still unanswered questions are: How many transmembrane helices can be fitted to the electron density of this domain? Is domain X membrane-buried or surface-exposed?

In conclusion, the stability of cytochrome oxidase is clearly dependent on the amphiphile used to solubilize the enzyme. The two main structural domains of the oxidase have different stabilities. Upon reduction of the enzyme, the domain formed by catalytic subunits I and II becomes more stable, while the stability of the other, less stable domain, composed primarily of subunit III, is independent of the redox-state. Subunit III does not contribute much to the stability of the oxidized enzyme. The transmembrane helices of the oxidase do not unfold thermally, and the denatured state of the enzyme may resemble the compact denatured state observed with soluble proteins under certain conditions [79].

4.3. The band 3 protein

In addition to transporting oxygen to tissues, red cells also participate in the elimination of CO_2, one of the end products of respiration. Part of this process is catalysed by the red cell anion transporter, designated the band 3 protein owing to its mobility in polyacrylamide gel electrophoresis in the presence of SDS (for recent reviews on the protein, see [165,208]). The band 3 protein (911 amino acids in human erythrocytes, M_r = 100 kDa, glycosylated at one Asn, acylated at one Cys and regulated by Tyr-phosphorylation at one main site), transports chloride or sulfate in exchange of bicarbonate; with SO_4^{2-}, a proton is cotransported. Glycosylation is not essential for function or folding [61]. The band 3 protein belongs to a family of related transporters all of which have a transmembrane part homologous to the band 3 transmembrane domain; these other members of the family occur in other tissues such as the kidney and the brain.

The band 3 protein is made up of two domains: The cytoplasmic domain carries binding sites for cytoskeletal proteins, glycolytic enzymes and hemoglobin, whereas the transmembrane domain performs the transport function. Although the domains can be separated by controlled proteolysis and are functional on their own [40,197], there is evidence for conformational interdomain interactions [12] and modulation of anion transport activity by ligand binding to the cytoplasmic domain [121]. The band 3 transmembrane domain has a molecular weight of 55 kDa

and catalyses anion transport with an activity similar to the native transporter. The transmembrane domain can be further cleaved to give 19 kDa and 35 kDa fragments which remain tightly associated and resistant towards guanidine hydrochloride denaturation [146].

The band 3 transmembrane domain is functional when expressed alone from a cDNA clone in *Xenopus* oocytes [61,114]. The same holds for the cytoplasmic domain produced in *E. coli* [229]. During its biosynthesis, band 3 protein may interact with glycophorin A, as coexpression of the latter increases the amount of band 3 protein in the plasma membrane [61,62]. However, direct evidence for a physical contact between mature band 3 protein and glycophorin A is scarce, suggesting that after translocation to the plasma membrane their interaction, if present, is weak [40,61]. Most of the ten introns in the portion of the human band 3 gene that encodes the transmembrane part occur in regions which are likely to be extramembranous [209]. This behavior is observed with some other membrane proteins [92], and has been taken to support the idea of transmembrane segments as independent folding domains [157].

The transmembrane domain of the band 3 protein is believed to contain 12 or 14 transmembrane spans, but biochemical evidence for this remains to be obtained [48,165]. In case there are 14 transmembrane spans in the membrane domain, some of them are expected to be fairly short, comprising only 14 or 15 residues (see [117,165,209]). Accordingly, it has been proposed that the actual physical permeability barrier inside the protein might be quite thin [209] (cf. [254]).

The estimates for α-helicity of the membrane domain range from 58% [146] to 69% [149]. In guanidine hydrochloride denaturation experiments, the ellipticity at 222 nm of the whole band 3 protein exhibits a biphasic dependence on the denaturant concentration with a large portion of the helicity still left at 4 M guanidine hydrochloride [146]. The isolated transmembrane domain is highly resistant towards the denaturant and does not fully unfold with guadinine concentrations experimentally accessible: at 4 M guadinine hydrochloride about 70% of the ellipticity at 222 nm is still observed.

In the red cell membrane, band 3 forms dimers which further associate to form tetramers. Monomers within a dimer appear to interact allosterically [176,222]. Since the isolated transmembrane domains are dimeric, dimerization appears to be mediated by the transmembrane domains while tetramer formation may require interactions between the cytoplasmic domains. Electron microscopic analysis of 2D crystals of the lipid-reconstituted transmembrane domain is consistent with a dimeric structure [230]. Further, the electron-microscopic work [230] allowed construction of a structural model of the domain at 20 Å resolution in which three subdomains within a monomer are resolved. One or two of the subdomains appear to have a different position relative to the other subdomains in the two crystal forms analyzed, indicating that there is some conformational flexibility within the domain. A 3D map determined from one of the crystal forms shows that the transmembrane domain of band 3 comprises a large basal part, situated inside the bilayer, and two sizable extramembrane parts on the cytosolic side of the membrane [254]. 2D crystals of the whole band 3 protein have also been reported [48]; despite the analysis of the crystals has yielded only a low resolution structure, a dimeric crystal packing unit appears likely.

Melting of both the cytoplasmic and transmembrane domains in situ give rise to separate peaks in calorimetric thermograms of the red cell membranes [18,27,40,197]. The transition of the membrane-bound cytoplasmic domain, designated the B_2 transition, is strongly pH dependent: its T_m shifts from 72°C at pH 6 to 55°C at pH 8.5 [27,197]. Unexpectedly, the isolated cytoplasmic fragment, although showing a similar pH dependence, is more stable than the domain in the native protein [27].

The transmembrane domain gives rise to a calorimetric peak at about 66–68°C (called the C transition) with a remarkable enthalpy change of 360–380 kcal/mol (6.7 cal/g), irrespective of whether the cytoplasmic domain is present or not [40,197]. The published specific ΔH value for the band 3 transmembrane domain is the largest among membrane proteins for which relevant data exists. The origin of this observation is not known even though several explanations can be put forth. Such a high value could be due to the melting of a significant portion of the intramembranous regions, however, this is not consistent with the CD data (see below). Alternatively, it could be an indication that not all the hydrophobic stretches identified in the hydropathy analysis are true transmembrane helices but form part of the extramembrane domain. The stability of such a domain is expected to resemble that of a soluble protein, undergo a relatively complete thermal unfolding and account for the relatively high enthalpy change. In this context, it should be noted that the exact number of transmembrane helices in band 3 is uncertain [165,209]. Of the 14 tentative transmembrane spans, the topology of the first eight appears to be fairly well-documented, whereas the folding pattern of the C-terminal half of the protein remains to be elucidated [208]. The recently published low-resolution 3D map of the membrane-bound part of band 3 shows that a significant portion of the molecule is extramembrane, although the author concluded that the intramembrane electron density could accommodate 12–14 transmembrane helices [254].

A third explanation for the high specific enthalpy change of band 3 transmembrane domain could involve a coupling to a lipid gel-to-fluid phase transition. A denaturation-linked decrease in the cross-sectional area of the protein is expected to decrease the amount of boundary lipid. The boundary lipid is known to be in a rigid gel-like configuration, and upon its liberation to the bulk fluid lipid environment of the bilayer a positive enthalpy contribution should

be observed (see Section 7.1). If this is true, the enthalpy change for band 3 denaturation should depend on the lipid chain length, as observed [123] (see below).

Within the context of the energetics of the C transition, it should also be noted that in some calorimetric studies the enthalpy of this transition appears much smaller after depletion of peripheral proteins (native membranes: 360 kcal/mol vs. 190 kcal/mol after removal of peripheral proteins (see [40,177]) suggesting some additional contributions to the measured enthalpy. A value of 190 kcal/mol (i.e., 3.5 cal/g) is more in line with the values observed with most other membrane proteins (see Fig. 10a).

Upon treatment of the membranes with the covalent anion transport inhibitor DIDS (4,4′-diisothiocyanostilbene-2,2′-disulfonic acid), the C transition shifts 10–13 degrees upwards [27,196,197,222]. By contrast, non-covalent inhibitors and membrane perturbants such as lidocaine and benzyl alcohol destabilize the transmembrane domain [19,41,196]; there is a quantitative relationship between the destabilization of the band 3 transmembrane domain and the inhibition of its anion transport activity by the local anesthetic lidocaine [41]. Also, delipidation of erythrocyte membranes by a phospholipase treatment or by the addition of fatty acids to the membranes results in a dramatic destabilization of the transmembrane domain, causing a total disappearance of the C transition [19,40]. The above results suggest that lipid–protein interaction makes a significant contribution to the stability of the tertiary structure of the band 3 transmembrane domain.

The stabilizing effect of DIDS [196], the pH dependence of the T_m of the cytoplasmic domain, the use of isolated domains generated by proteolysis as well as the differential sensitivity of the cytoplasmic and transmembrane domains towards chemical denaturation has allowed the calorimetric measurement of one transition in the absence of the other [7,40]. As discussed already, it appears that there is little cross-talk between the B_2 and C transitions and it was therefore concluded that the two domains are largely independent of each other. However, subtle interdomain interactions have been detected by other techniques [12,121,165].

What are the molecular changes that take place when the temperature is scanned over the region in which the C transition occurs? In an early study, Brandts et al. [18] monitored the CD of red cell membranes as a function of temperature and observed no changes in the secondary structure during the C transition; the authors concluded that the transition is unlikely to involve protein unfolding. However, using the purified band 3 transmembrane domain, Davio and Low [40] definitely assigned the C transition to the band 3 protein but they also found 70% of the ellipticity to be insensitive towards raising the temperature above the transition region [40]. This suggests that the majority of transmembrane helices do not unfold thermally, in agreement with the notion that the α-helical secondary structure of the transmembrane domain is remarkably resistant towards chemical denaturation by guadinine hydrochloride [146]. To summarize, these results suggest that the major event during the C transition is the disruption of interhelical contacts and unfolding of extramembrane parts of the protein while the transmembrane helices themselves remain largely folded.

Results that support this idea have been obtained with a variant band 3 found in individuals with Southasian ovalocytosis (SAO). This condition is characterized by a highly distinctive red cell morphology and altered mechanical properties of the cells [209]. Recent research suggest that SAO is caused by a nine-residue deletion at the cytoplasmic boundary of the first transmembrane segment of band 3 [91,185]. The deletion includes a proline residue that is likely to occupy a critical position at the N-terminal end of the helix, and this has been proposed to be responsible for the folding defect of the whole transmembrane domain [132,186]. Normal amounts of band 3 protein are present in SAO individuals but about 50% of the protein is inactive and abnormally glycosylated [178]. The deletion seems not to affect the cytoplasmic domain [135]. Significantly, the ΔH of the C transition in the SAO red cell membranes is only 55% of controls, suggesting that the SAO variant does not contribute much to the enthalpy [135]. Further experiments showed that the enthalpy of the SAO band 3 transmembrane domain is about 8% of the wild type. Nevertheless, the SAO variant and normal band 3 proteins have a similar, largely α-helical secondary structure [135,178]. The fact that a nine residue deletion does cause a loss of the tertiary structure of the whole transmembrane domain suggests that in the native structure of the band 3 protein the helices are organized in a highly cooperative fashion.

Interestingly, in SAO membranes the T_m of the C transition of those band 3 molecules which do not carry the deletion is lowered by 2°C [135]. It seems that the SAO band 3 molecules slightly destabilize their normal neighbors in the membrane, perhaps as a result of altered interactions in a heterotetramer formed by the SAO and normal band 3 homodimers [135].

The stability of the purified band 3 transmembrane domain in different lipid environments has been studied in detail by Maneri and Low [123]. The length of the acyl chains, the amount of double bonds in them as well as the charge of the headgroup all have a clear effect on the thermotropic behavior of the domain. There is a linear relationship between the acyl chain length and the T_m: in mono-unsaturated phosphatidylcholine vesicles, the T_m increases from 47°C with 14-carbon acyl chains to 66°C with 24-carbon fatty acids. The corresponding enthalpies, however, exhibited a maximum of about 400 kcal/mol (7.3 cal/g) with 20-carbon fatty acids. The band 3 transmembrane domain is most stable when reconstituted with cholesterol plus phospholipids containing saturated fatty acids and zwitterionic head groups. This preference for long and saturated acyl chains is also reflected in the

endogeneous lipid content of the purified transmembrane domain (6–7 mol lipid/mol of transmembrane domain [123]. When reconstituted in mono-unsaturated zwitterionic lipids with or without cholesterol (at a protein-to-lipid mass ratio of 1:3), a ΔC_p of about 8 kcal/mol K was observed; this is close to the value expected for a soluble protein of similar size. In contrast, increasing the degree of unsaturation or use of negatively charged lipids resulted in a very small or negative ΔC_p [123].

The stabilities of the detergent solubilized band 3 and of the isolated transmembrane domain have also been studied [177]. None of the detergents used were able to restore the enthalpy measured for the membrane-bound band 3 and also the T_m values were lower. The isolated transmembrane domain had a significantly lower T_m than the whole protein, although enthalpies appeared comparable. The stability was clearly highest (i.e., the T_m was highest; cf. [123]) when the protein was dispersed in poly(oxyethylene) detergents with a 12-carbon chain or in Triton X-100, all of which yielded ΔH values of 200–300 kcal/mol and scanning rate dependent T_m values close to 61°C with the scan rate used [177].

The results of both Sami et al. [177] and Maneri and Low [123] suggest that optimal matching between the length of a transmembrane helix and the length the hydrocarbon chain of the amphiphile plays a role in the stabilization of a membrane protein (see also [136,245]).

4.4. Photosystem II

Photosystem II (PS II) is a complex membrane protein assembly that catalyses the water-splitting reaction and the associated electron transfer reactions in oxygenic photosynthesis (for a review, see [11]). The PS II complex of plants contains at least 25 polypeptides [5,11] (see Fig. 9). A detergent treatment splits it into two parts, called the core fraction and the antenna fraction. The core fraction of PS II comprises approximately 15 polypeptides, of which three are located peripherally on the lumenal side of the thylakoid membrane. One of the peripheral proteins (a 33 kDa polypeptide) stabilizes the tetranuclear manganese cluster which is the site of water splitting and oxygen generation. However, the ligands of the manganese cluster are probably located in two lumenal loops of the D_1 subunit which is one of the two major intrinsic membrane proteins of the core. These two proteins, designated D_1 and D_2, are weakly homologous to the L and M subunits of the bacterial photoreaction center. Most probably, D_1 and D_2 perform a function analogous to the L and M polypeptides in the bacterial system. A subcomplex of D_1, D_2 and a *b*-type cytochrome has in fact been shown to be capable of catalysing the light driven charge separation that makes up the first step of photosynthesis [45].

The main component of the antenna fraction are the light-harvesting chlorophyll *a/b* binding proteins, which are a group of similar but not identical proteins. A structural model of a light-harvesting protein at 3.4 Å resolution, showing a supercoil of two parallel transmembrane helices, a third separate transmembrane helix and locations of 12 chlorophyll and two lutein molecules, has been published [105]. The three transmembrane helices comprise 36% of the 232 residues in the polypeptide.

The chlorophylls are mostly located in the periphery of the trimeric complex; the axial ligands of most of them are

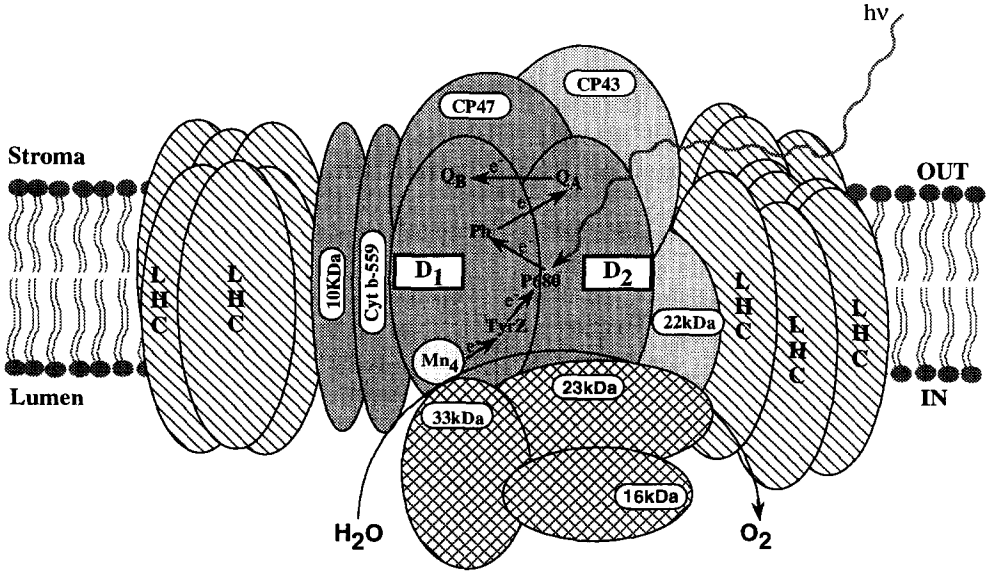

Fig. 9. A model depicting the structure of PS II in the thylakoid membrane of chloroplasts. Only the major subunits of the core and the antenna are shown. Subunits melting during each calorimetric transition are indicated by different hatching (for details see the text). The assignment of the 33 kDa, 23 kDa and 16 kDa peripheral proteins to the A_2 transition is tentative, as no protein precipitation is observed during this transition. Note the location of the oxygen evolving center close to the inside of the membrane. LHC, light-harvesting complex. Adapted from [5].

resolved in the structural model of Kühlbrandt et al. [105]. About 30% of the mass of the light-harvesting complex is chlorophyll molecules, which are therefore thought to play a significant role in the structural stability of the protein [88]. A structural role is also postulated for the two long lutein molecules which seem to 'cross-link' the two supercoiled helices. The lutein molecules (xanthophylls) have been shown to be essential for the in vitro reconstitution of the light-harvesting complex [151,258]. Bound lipid is of structural importance as well [145].

As expected from its polypeptide composition, the thermogram of PS II is complex, exhibiting at least four transitions (A_2, B, C, D) in the 40–70°C temperature range [35,212,213]. The total calorimetric enthalpy change of the whole PS II complex (including both the core and the antenna) is about 3300 kcal/mol (5–6 cal/g) [212], assuming a molecular mass of 600 kDa (which may be an underestimate).

Thermal gel analysis, heat inactivation studies and DSC of the isolated core and antenna fractions suggest that the low temperature transition (A_2 at 47.5°C) is caused by denaturation of a component involved in oxygen evolution [213]. No protein precipitation was observed during the transition. This result suggests that the transition might be brought about by a soluble protein, such as the 33 kDa extrinsic protein which stabilizes the oxygen evolving Mn cluster. Two of the four manganese atoms in the complex are released when the temperature is scanned over the transition [35]. The cooperativity of the A_2 transition appears to be strongly influenced by the redox state of the *b*-type cytochrome (which itself denatures at a temperature clearly higher, see below), suggesting that the membrane-bound cytochrome influences the structure of the oxygen evolving complex. The cytochrome is required for the stable assembly of the PS II complex [147].

Transition B (54°C) has contributions from core proteins referred to as closely associated antenna proteins or chlorophyll *a* binding proteins as well as some other intrinsic membrane proteins which belong to the PS II core [11,213]. Loss of electron transfer activity occurs during the B transition. The C transition (59.5°C) is sensitive to Mg^{2+} and corresponds to the denaturation of the major components of the core, the D_1, D_2 and the *b*-type cytochrome. The light-harvesting complex proteins, being the most stable, give rise to the high temperature peak D at 66°C. Taken together, these studies suggest that PS II is composed of four structural units, one peripheral and three membrane-bound [213] (see Fig. 9). The least stable part of the complex appears to be the O_2-evolving part, thought to be located on the lumenal side of the thylakoid membrane [5].

The thermogram of PS II is very sensitive to the detergent concentrations used: increasing the concentration of Triton X-100 from 0.01% to 0.1% results in substantial broadening of the DSC peaks, and some transitions, such as peak D caused by the light-harvesting proteins, are broadened almost beyond detection [212]. Hence, the interactions between PS II subunits appear not to be as strong as those of most other proteins, i.e., subunit dissociation and/or loss of cooperative interactions take place upon increasing the detergent concentration [259]. A recent re-

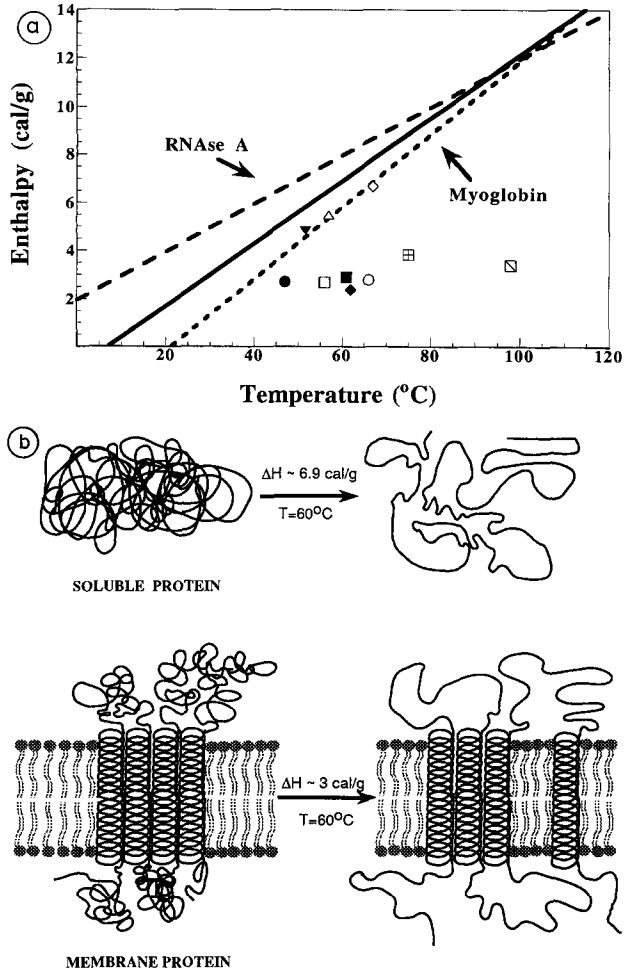

Fig. 10. (a) Comparison of the calorimetric enthalpies (cal/g) of the membrane proteins discussed in the text with an average soluble protein (—), with a protein having a highly hydrophobic core (myoglobin, —) and with a protein having a relatively hydrophilic core (RNAse A,——). Membrane proteins: Photosystem II (△); the band 3 protein (◇); monomeric bacteriorhodopsin (⊞); trimeric bacteriorhodopsin in the purple membrane (⋆); *Paracoccus denitrificans* cytochrome-*c* oxidase subunit III (●); *P. denitrificans* cytochrome-*c* oxidase (wild type; weighted mean of the two transition temperatures) (■); *P. denitrificans* cytochrome oxidase purified from the subunit III-minus mutant (○); cytochrome-*c* oxidase from beef (□); subunit III of beef cytochrome-*c* oxidase (▼); cytochrome-*c* oxidase from yeast (◆). Note the low enthalpies of denaturation of most membrane proteins. For references see the text. (b) A schematic model of the thermal denaturation of a helical membrane protein. A likely explanation for the low enthalpy changes is the high thermal stability of a transmembrane α-helix. As a result, transmembrane helices do not unfold, contrary to the situation with a soluble protein or the extramembrane domain of a membrane protein. Also illustrated in the figure is the possibility that packing interactions among transmembrane helices are only partially disrupted in the denatured state. Approximate experimental enthalpy values at 60°C are given. For further discussion and references, see the text.

port suggests that in the pea chloroplast light-harvesting complex, there are specific lipid binding sites which must be occupied by phosphatidyl glycerol in order to preserve the trimeric structure of the complex [145]. In addition, about three molecules of digalactocyl diacyl glycerol per light-harvesting protein complex monomer are required for the formation of 2D or 3D crystal lattices. This requirement is also likely to reflect the existence of structurally important lipid binding sites [145,258].

Fig. 10 summarizes the calorimetric behavior of the proteins discussed above and compares their energetics to that of soluble proteins.

4.5. Porins

Porins (see Fig. 1f) are channel-forming proteins found in the outer membrane of gram-negative bacteria where they facilitate the diffusion of molecules smaller than 600 Da into and from the periplasm (for reviews, see [31,142,143,188]. Although no quantitative thermodynamic measurements with porins have been reported so far, the recent elucidation of the atomic structures of four porins [32,104,233] warrants a brief discussion of their structural stability here, in particular because porins appear to be exceptionally stable proteins.

Despite being integral membrane proteins, porins do not have hydrophobic primary structures; nor do they contain hydrophobic sequences typical of transmembrane α-helices. Another interesting feature is that, although having similar gross 3D structures [32,233], the *Rb. capsulatus* porin and the two homologous *E. coli* porins (OmpF and PhoE) have rather different amino acid sequences with no overall sequence homology [183]. This fact makes it difficult to predict without additional information whether a novel sequence really codes for a porin or other membrane protein with similar characteristics.

The X-ray structures show that a porin molecule is a trimer, as expected from biochemical analyses. Each monomer comprises a barrel made up of 16 antiparallel β-strands surrounding an aqueous channel along which solutes enter or exit the periplasm [32,233] (Fig. 1f). Access to the channel from the outside is controlled by one interstrand loop that folds into the pore, limiting its size ('the eyelet') [188]. The membrane-buried part of porin is composed solely of non-polar β-sheet surface; as mentioned earlier, aromatic residues are enriched at both lipid-aqueous interfaces, forming two aromatic 'girdles' [32,187,233,234]. In these aromatic zones phenylalanines are located toward the lipid core whilst tyrosine hydroxy groups and tryptophans point toward the lipid headgroups. The non-polar part (including the aromatic girdles) of the porins is 24–25 Å wide [32,233]. In the *Rb. capsulatus* porin ($M_{r,monomer}$ = 32 kDa) 50 of the 301 residues in the protein make up this hydrophobic surface [188]. Thus the majority of the residues are exposed to aqueous phase (166 residues) or participate in intermonomeric contacts (85 residues) [188]. The loops connecting the β-strands on the periplasmic side are very short and contain polar (and non-charged in *Rb. capsulatus*) residues in hydrogen-bonded reverse turns whereas the longer external loops are rich in charged amino acids and fold into more complex structures including three short α-helices [233].

The porin trimer is highly stable: it is denatured by SDS only at temperatures close to 100°C and it is resistant against many proteinases [52]. Three structural factors appear to play pivotal roles in the stability of the porin trimer: (i) the extensive hydrogen bonding in the β-barrel (ii) the rigid and structured loops on both sides of the membrane (iii) the strong interaction between the monomers.

In the *Rb. capsulatus* porin structure at 1.8 Å resolution, the β-barrel comprises 178 residues which form a total of 161 hydrogen bonds [233]. The crystallographic temperature factors show that the barrel is the most rigid part of the molecule. Most of the loops have also low temperature factors, indicating that they are highly structured. In particular, the long loop that constricts the mouth of the channel (the eyelet) is rigid, being stabilized by salt bridges and also by two bound calcium ions in *Rb. capsulatus* porin [233]. The differences in the barrel shape between the two *E. coli* porins and the *Rb. capsulatus* porin may owe to the differences in the loop structures [32]. The charged external parts may be further stabilized by polar interactions with the lipopolysaccharide, present in the outer leaflet of the outer membrane [142,188].

As indicated by the crystallographic temperature factor, the most ordered part of the *Rb. capsulatus* porin trimer is made up of the regions that are involved in the intermonomer contacts [233]. Both optimal packing interactions that involve many phenylalanine residues and polar interactions (hydrogen bonds) are important for the structure, as is a third calcium ion chelated between the neighboring monomers [233]. 28% of the residues in the *Rb. capsulatus* porin monomer are located in the interface region and an area of 8120 Å^2 is buried upon trimerization, forming the hydrophobic core of the trimer [188,233]. The accessible surface areas of the porin monomer and trimer appear to follow the same dependence on the molecular mass as observed with soluble proteins (unpublished results from this laboratory). In the *E. coli* porins, aromatic and small residues form complementary surfaces that pack optimally against each other at the interface [32]. In addition, the salt-bridged termini of each monomer are located in the interface region [32,187].

Although the assembly pathway of porins is not known, it is possible that after translocation to the periplasm, a porin monomer adopts a metastable water-soluble conformation [144]. Schulz [187] has suggested that the folding of a porin *trimer* begins in the aqueous phase with the formation of the trimer interface which in the crystal structure resembles the hydrophobic core of soluble proteins. The interface contains all the six termini of the three

polypeptide chains; the last C-terminal strand and its last residue in particular (a well conserved Phe) have been shown to be critical for the folding process [142]. This step is then followed by the membrane insertion step which would induce the formation of the hydrogen bond network of the surrounding β-barrel. The final stage of folding would include the stabilization of the transmembrane barrel by formation of the external loops. This process might be assisted by interaction of the loops with the lipopolysaccharide.

The latter suggestion is in agreement with the observation that a porin trimer (but not a monomer) binds lipopolysaccharide molecules with a high affinity [52]. Also, efficient refolding of denatured monomeric porin [2] back to trimers appears to require an SDS-like amphiphile with sulfate or sulfonate groups; in the presence of non-ionic or cationic detergents refolding is much less efficient [52]. As an explanation for this finding, it has been proposed that SDS mimics the physiological action of lipopolysaccharide [142,143]. This would also explain why the porins tolerate SDS exceptionally well. In this context, it is interesting that several bound detergent molecules are seen in the crystal structures [104,233].

5. Consensus behavior

A recurring theme in the above discussion is the very high stability of the transmembrane domains of membrane proteins as compared to their extramembrane parts or to soluble proteins. Apparently only the extramembrane portions undergo significant thermal unfolding, and the observed enthalpies of denaturation are therefore very low (see Fig. 10 for a summary of the preceding discussion).

The immersion of a peptide into the lipid bilayer provides a means of achieving a remarkably thermostable structure. In a transmembrane protein, the least stable parts are generally the loops connecting the transmembrane domains and the extramembranous regions. On the other hand, transmembrane helices appear not to undergo thermal denaturation in most membrane proteins studied. As exemplified by bacteriorhodopsin and the porins, a very thermostable overall structure is possible, even in organisms which are not thermophiles. The early Earth was probably warmer than our planet is today [241,242], and thermostability was probably a necessary property of primordial proteins. Thus it is conceivable that spontaneous generation of lipid bilayer vesicles and the subsequent, spontaneous insertion of thermostable helical peptides (see also [251]) into the bilayer have been crucial events in the early development of life.

[2] Unlike helical membrane proteins, porin seems to adopt a random coil configuration in 6 M guadinine hydrochloride.

6. The structural stability of membrane proteins

As discussed above, the process measured in thermal denaturation studies of membrane proteins is not a transition from the native state of the protein to a disordered polypeptide chain, but rather a transition from the native state to a denatured state which is generally still associated to the membrane or to a detergent micelle, has different degrees of residual structure and in some cases different degrees of intermolecular aggregation. According to the existing data, thermal denaturation affects primarily the extramembrane regions, while the transmembrane regions very likely retain most of their secondary structure and perhaps most of their packing interactions. The energetics of the regions exposed to water are likely to reflect forces similar to those operative in water soluble proteins. In addition, interactions with the headgroup region of the membrane might influence their energetics.

7. Thermodynamics of protein stability

7.1. The Gibbs free energy function of extramembrane regions

Under equilibrium conditions the stability of the native state of a protein is determined by its relative Gibbs free energy (ΔG). In turn, the Gibbs free energy is a function of three quantities, the relative enthalpy (ΔH), entropy (ΔS) and heat capacity (ΔC_p):

$$\Delta G = \Delta H(T_R) + \Delta C_p[T - T_R] - T\left[\Delta S(T_R) + \Delta C_p \ln[T/T_R]\right] \quad (1)$$

where T_R is some appropriate reference temperature. In this article we follow the standard convention and use the native state as the reference state for all thermodynamic parameters.

For water soluble globular proteins or those regions of membrane proteins that become exposed to water upon denaturation, the enthalpy and entropy changes are temperature dependent and as a result, the Gibbs free energy becomes a non-linear function of temperature. This is due to the existence of a positive ΔC_p resulting from the exposure to water of hydrophobic residues that are not accessible to solvent in the native structure [160].

The solvent accessible surface area (ASA) of a protein can be divided into polar and apolar components which can be determined by a number of algorithms using the 3D structure of the protein (see [38,137]). The heat capacity change is directly proportional to the change in polar and apolar solvent accessible surface between conformations [137,138]:

$$\Delta C_p = \Delta \mathrm{ASA}_{ap}\, \Delta C^o_{p,ap} + \Delta \mathrm{ASA}_{pol}\, \Delta C^o_{p,pol} \quad (2)$$

where ΔASA_{ap} and ΔASA_{pol} represent the change in accessible apolar and polar surface area respectively and $\Delta C^{o}_{p,ap}$ and $\Delta C^{o}_{p,pol}$ the elementary ΔC_p contributions per mole of Å^2. $\Delta C^{o}_{p,ap}$ and $\Delta C^{o}_{p,pol}$ have been estimated as 0.45 ± 0.02 cal K^{-1}(mol Å^2)$^{-1}$ and -0.26 ± 0.03 cal K^{-1}(mol Å^2)$^{-1}$. It must be noted that other effects appear to contribute very little to the observed ΔC_p.

The bulk of the enthalpy change can also be expressed as a linear combination of the changes in polar and apolar solvent accessible surface areas (ASA):

$$\Delta H(T) = a(T)\,\Delta ASA_{ap} + b(T)\,\Delta ASA_{pol} \quad (3)$$

$$\Delta H(T) = a(T_R)\,\Delta ASA_{ap} + b(T_R)\,\Delta ASA_{pol} + \Delta C_p(T - T_R) \quad (3a)$$

where T_R is an appropriately chosen reference temperature. The reference temperature is chosen as 60°C [248], which corresponds to the median transition temperature for the proteins in the database. (The thermodynamic-structural database consists of proteins for which both high resolution structural model and accurate thermodynamic information exists [138,248].) This choice minimizes extrapolation errors due to uncertainties in ΔC_p and the possibility that ΔC_p for some proteins might not be constant [161]. At 60°C the enthalpy change can be written as:

$$\Delta H(60) = 31.4\Delta ASA_{pol} - 8.44\Delta ASA_{ap} \quad (4)$$

At the reference temperature, the average error between the experimental and calculated values is 6%. Under most conditions, Eqs. (2) and (3) account for over 90% of the enthalpy change of unfolding. The additional terms correspond mainly to the enthalpies associated with protonation or the effects of specific ligands, if present. Those additional contributions need to be taken into account explicitly, especially at low temperatures in which the contribution given by Eq. (2) is close to zero. The protonation of carboxylic groups has an enthalpy close to -1 kcal mol^{-1} and that of histidyl groups is close to -7 kcal mol^{-1}.

Very little, if anything, is known about the energetic contributions of the intramembranous regions. For these or other regions that undergo denaturation without exposure to water the ΔC_p is expected to be negligible. Since transmembrane helices do not appear to undergo melting inside the membrane, their enthalpic contributions during thermal denaturation could be limited mostly to van der Waals contributions due to changes in their packing as well as effects related to lipids. The magnitude of the enthalpic contributions due to packing changes in transmembrane helices is currently unknown. Regarding the lipids, Nagle and Wilkinson [140] theoretically estimated that the van der Waals contribution to the gel–liquid crystalline transition of lipid molecules is on the order of 0.15–0.2 kcal per mole of CH_2. It has been known for many years that the presence of a membrane protein affects the physical state of lipid molecules directly in contact with the protein [136]. Therefore changes in the cross-sectional areas of membrane proteins induced by thermal denaturation will induce changes in the number of lipid molecules affected by this interaction and a concomitant enthalpic contribution. This protein lipid contribution (ΔH_{pl}) can be written as:

$$\Delta H_{pl} = \Delta N_{pl}\,\Delta h_{pl} \approx 2\pi\Delta R_p\,\Delta h_{pl}/R_l$$

where ΔN_{pl} is the change in the number of lipid molecules interacting with the protein upon denaturation and Δh_{pl} the enthalpy contribution per mol of lipid molecule. If the cross section of the protein is assumed to be circular then ΔN_{pl} can be approximated in terms of the change in protein radius ΔR_p and the radius of the lipid molecule R_l. If the bulk of the membrane is in the fluid state Δh_{pl} can be reasonably expected to be positive. Also, Δh_{pl} is expected to increase with chain length and to depend on other factors known to affect the enthalpy of the gel–liquid crystalline transition. At the present time very little is known regarding the magnitude of the enthalpic changes contributed by the intramembranous regions of proteins. Systematic studies of proteins with known structures are needed to address this issue.

7.2. The entropy change

Baldwin [10] showed that at 112°C the entropy associated with the dissolution of apolar substances in water is nearly zero. At this same temperature, the average entropy change for the unfolding of water soluble globular proteins, after correction for protonation and ligand effects, has been recently shown to correspond to the configurational entropy change associated with the change in degrees of freedom of the backbone and of the side chains. At any temperature, the entropy change can be written as:

$$\Delta S(T) = \Delta S(112) + \left[\Delta C_{p,pol} + \Delta C_{p,ap}\right]\ln[T/385.15] \quad (4)$$

Since, experimentally, the protein unfolding entropy change at 112°C corresponds to the conformational entropy change and it is known that the apolar contribution to ΔS is zero at this temperature [10,139], it follows that other contributions such as polar, vibrational, etc. are either negligible or cancel each other. For water-soluble proteins in the thermodynamic database, $\Delta S(112)$ is equal to 4.3 ± 0.2 cal K^{-1} (mol res)$^{-1}$. This figure is an average for all amino acids weighted according to their proportion in the database, and includes configurational entropy changes from the backbone and from the side chains. However, the average value is too coarse an estimate to be used successfully to predict effects of site-directed mutagenesis on T_m, for instance.

It has been proposed [59] that the configurational entropy could be written in terms of a minimum of three different types of contributions: (i) $\Delta S_{bu \rightarrow ex}$, the entropy

change associated with the transfer of a side chain that is buried in the interior of the protein to its surface; (ii) $\Delta S_{ex \rightarrow u}$, the entropy change gained by a surface exposed side chain when the peptide backbone unfolds; and, (iii) ΔS_{bb}, the entropy change gained by the backbone itself upon unfolding. Consequently, as a first approximation, the total entropy change can be written as:

$$\Delta S_{conf} = \sum_i \Delta S_{ex \rightarrow u,i} + \sum_j \Delta S_{bu \rightarrow ex,j} + \Delta S_{bb} \quad (5)$$

where the summation i runs over all amino acid side chains and the summation j runs only over those amino acids that are buried. The backbone entropy is a function of the length of the peptide chain, the amino acid composition and the presence of disulfide bridges or other covalent bonds in the backbone. As a first approximation, the value of $\Delta S_{ex \rightarrow u,i}$ can be equated to the side chain entropy change associated with a helix-to-coil transition. Recently, Creamer and Rose [37] estimated side chain contributions to the configurational entropy change of helix-to-coil transitions in isolated peptides using Monte Carlo simulations. According to their study, the average side chain contribution for the amino acids studied (Ile, Leu, Met, Phe, Trp, Tyr, Val) is on the order of 0.74 cal K^{-1} mol^{-1}. This value is close to the one derived previously by Nemethy et al. [141] (0.5 cal K^{-1} mol^{-1}). Creamer and Rose [37] calculated also the configurational entropy of side chains in the α-helix, which ranges between 0.2 and 4.7 cal K^{-1} mol^{-1}, the average being 2.8 ± 1.7 cal K^{-1} mol^{-1} for the amino acids studied. If it is assumed that the side chains buried in the interior of the protein have zero configurational entropy, then those entropy values can be considered to approximate the configurational entropy change of transferring a side chain from the interior of the protein to its surface. Finally, in the absence of covalent links, the backbone entropy is primarily a function of the steric hindrances imposed by the side chains on the rotational degrees of freedom of the peptide chain. This entropy term is maximal for glycine, it decreases rather dramatically for alanine and continues to decrease for larger side chains. At the present time no accurate estimates for these contributions are available. It has been estimated that glycine should contribute around 5.5 cal K^{-1} mol^{-1} and that this value should drop to about 3 cal K^{-1} mol^{-1} for alanine [141]. The partitioning described by Eq. (5) provides a more accurate estimation of the configurational entropy than the simple average ΔS^* value. The values for $\Delta S_{ex \rightarrow u}$ and $\Delta S_{bu \rightarrow ex}$ for all twenty amino acids except proline have been estimated by Lee et al. [109]. These results are summarized in Table 1.

In membrane proteins, the unfolding of the extramembranous portions is expected to be associated with conformational entropy changes similar to those existing in water soluble proteins, although in some cases the highly stable transmembrane part might restrict unfolding of an extramembrane part. These restrictions will decrease the entropy of the denatured state and contribute to the stabilization of the native state. By contrast, the situation regarding the entropy change is quite different for the intramembranous regions. At the present time almost nothing is known concerning the degrees of freedom of amino acid side chains exposed to the lipid bilayer. Do they have the same degrees of freedom as side chains exposed to water? Does the peptide backbone inside a bilayer have significant conformational freedom? Are there any significant conformational entropy contributions from transmembrane regions to the denaturational entropy? These and other questions discussed in this article will need to be answered before a thorough understanding of the energetics of membrane proteins can be achieved.

Table 1
Conformational entropies for amino acids

Amino acid	$\Delta S_{bu \rightarrow ex}$ (cal/K mol)	$S_{ex \rightarrow u}$ (cal/K mol)	ΔS_{bb} (cal/K mol)
Ala	0.00	0.00	2.1
Arg	7.11	−0.84	≈1.6
Asn	3.29	2.24	≈1.6
Asp	2.00	2.16	≈1.6
Cys	3.55	0.61	≈1.6
Gln	5.02	2.12	≈1.6
Glu	3.53	2.27	≈1.6
Gly	0.00	0.00	4.8
His	3.44	0.79	≈1.6
Ile	1.74	0.67	<1.6
Leu	1.63	0.25	≈1.6
Lys	5.86	1.02	≈1.6
Met	4.55	0.58	≈1.6
Phe	2.78	1.51	≈1.6
Ser	3.68	0.55	≈1.6
Thr	3.31	0.48	≈1.6
Trp	2.74	1.15	≈1.6
Tyr	4.16	1.74	≈1.6
Val	0.12	1.29	<1.6

$\Delta S_{bu \rightarrow ex}$ and $\Delta S_{ex \rightarrow u}$ are from Lee et al. [109]. Values for ΔS_{bb} are approximations estimated from Nemethy et al. [141] (see Lee et al. [109] for details).

Acknowledgements

Supported by grants GM3791 and RR04328 from the National Institutes of Health. T.H. thanks the Finnish Cultural Fund and the Magnus Ehrnrooth Foundation for travel grants.

References

[1] Abrahams, J.P., Lutter, R., Todd, R.J., Van Raaij, M.J., Leslie, A.G.W. and Walker, J.E. (1993) EMBO J. 12, 1775–1780.
[2] Adams, G.A. and Rose, J.K. (1985) Cell 41, 1007–1015.
[3] Allen, J.P., Feher, G., Yeates, T.O., Komiya, H. and Rees, D.C. (1987) Proc. Natl. Acad. Sci. USA 84, 5730–5734.
[4] Altenbach, C., Marti, T., Khorana, H.G. and Hubbel, W.L. (1990) Science 248, 1088–1092.

[5] Andersson, B. and Franzen, L.-G. (1992) in Molecular Mechanisms in Bioenergetics (Ernster, L., ed.), New Comprehensive Biochemistry, Vol. 23, pp. 121–143, Elsevier, Amsterdam.
[6] Andersson, H. and Von Heijne, G. (1994) EMBO J. 13, 2267–2272.
[7] Appell, K.C. and Low, P.S. (1982) Biochemistry 21, 2151–2157.
[8] Arrondo, J.L.R., Castresana, J., Valpuesta, J.M. and Goni, F.M. (1994) Biochemistry 33, 11650–11655.
[9] Baldwin, J.M. (1993) EMBO J. 12, 1693–1703.
[10] Baldwin, R.L. (1986) Proc. Natl. Acad. Sci. USA 83, 8069–8072.
[11] Barber, J. and Andersson, B. (1992) Trends Biochem. Sci. 17, 61–66.
[12] Batenjany, M.M., Mizukami, H. and Salhany, J.M. (1993) Biochemistry 32, 663–668.
[13] Bianchet, M., Ysern, S., Hullihen, J., Pedersen, P.L. and Amzel, L.M. (1991) J. Biol. Chem. 266, 21197–21201.
[14] Blobel, G. (1980) Proc. Natl. Acad. Sci. USA 77, 1496–1500.
[15] Bormann, B.J., Knowles, W.J. and Marchesi, V.T. (1989) J. Biol. Chem. 264, 4033– 4037.
[16] Braiman, M.S., Stern, L.J., Chao, B.H. and Khorana, H.G. (1987) J. Biol. Chem. 262, 9271–9276.
[17] Brandl, C.J. and Deber, C.M. (1986) Proc. Natl. Acad. Sci. USA 83, 917–921.
[18] Brandts, J.F., Erickson, L., Lysko, K., Schwartz, A.T. and Taverna, R.D. (1977) Biochemistry 15, 3450–3454.
[19] Brandts, J.F., Taverna, R.D., Sadasiwan, E. and Lysko, K.A. (1978) Biochim. Biophys. Acta 512, 566–578.
[20] Brouillette, C.G., Muccio, D.D. and Finney, T.K. (1987) Biochemistry 26, 7431–7438.
[21] Brouillette, C.G., McMichens, R.B., Stern, L.J. and Khorana, H.G. (1989) Proteins 5, 38–46.
[22] Cao, H., Bangalore, L., Bormann, B.J. and Stern, D.F. (1992) EMBO J. 11, 923–932.
[23] Capaldi, R.A. (1990) Arch. Biochem. Biophys. 280, 252–262.
[24] Castresana, J., Lübben, M., Saraste, M. and Higgins, D.G. (1994) EMBO J. 13, 2516–2525.
[25] Caughey, W.S., Dong, A., Sampath, V., Yoshikawa, S. and Zhao, X.-J. (1993) J. Bioenerget. Biomembr. 25, 81–91.
[26] Chang, C.-H., El-Kabbani, O., Tiede, D., Norris, J. and Schiffer, M. (1991) Biochemistry 30, 5352–5360.
[27] Chepuri, V. and Gennis, R.B. (1990) J. Biol. Chem. 265, 12978–12986.
[28] Chothia, C. (1984) Annu. Rev. Biochem. 53, 1537–1572.
[29] Cosson, P. and Bonifacino, J.S. (1992) Science 258, 659–662.
[30] Cosson, P., Lankford, S.P., Bonifacino, J.S. and Klausner, R.D. (1991) Nature 351, 414–416.
[31] Cowan, S.W. (1993) Curr. Opin. Struct. Biol. 3, 501–507.
[32] Cowan, S.W., Schirmer, T., Rummel, G., Steiert, M., Ghosh, R., Pauptit, R.A., Jansonius, J.N. and Rosenbusch, J.P. (1992) Nature 358, 727–733.
[33] Cowan, S.W. and Rosenbusch, J.P. (1994) Science 264, 914–916.
[34] Cramer, W.A., Martinez, S.E., Huang, D., Tae, G.-E., Everly, R.M., Heymann, J.B., Cheng, R.H., Baker, T.S. and Smith, J.L. (1994) J. Bioenerget. Biomembr. 26, 31–47.
[35] Cramer, W.A., Whitmarsh, J. and Low, P.S. (1981) Biochemistry 20, 157–162.
[36] Cramer, W.A., Engelman, D.M., Von Heijne, G. and Rees, D.C. (1992) Faseb J. 6, 3397–3402.
[37] Creamer, T.P. and Rose, G.D. (1992) Proc. Natl. Acad. Sci. USA 89, 5937–5941.
[38] Creighton, T.E. (1993) Proteins–Structures and Molecular Properties, W.H. Freeman, New York.
[39] Creighton, T.E. (1991) Curr. Opin. Struct. Biol. 1, 5–16.
[40] Davio, S.R. and Low, P.S. (1982) Biochemistry 21, 3585–3593.
[41] Davio, S.R. and Low, P.S. (1982) Arch. Biochem. Biophys. 218, 421–428.
[42] Davis, N.G., Boeke, J.D. and Model, P. (1985) J. Mol. Biol. 181, 111–121.
[43] Deatherage, J.F., Henderson, R. and Capaldi, R.A. (1982) J. Mol. Biol. 158, 501–514.
[44] Degli Esposti, M., Crimi, M. and Venturoli, G. (1990) Eur. J. Biochem. 190, 207–219.
[45] Deisenhofer, J. and Michel, H. (1991) Annu. Rev. Cell Biol. 7, 1–23.
[46] Dempsey, C.E. (1992) Biochemistry 31, 4705–4712.
[47] De Vos, A.M., Ultsch, M and Kossiakoff, A.A. (1992) Science 255, 306–312.
[48] Dolder, M., Walz, T., Hefti, A. and Engel, A. (1993) J. Mol. Biol. 231, 119–132.
[49] Donnelly, D. and Codgell, R.J. (1993) Protein Eng. 6, 629–635.
[50] Donnelly, D., Overington, J.P., Ruffle, S.V., Nugent, J.H.A. and Blundell, T.L. (1993) Protein Sci. 2, 55–70.
[51] Durell, S.R. and Guy, H.R. (1992) Biophys. J. 62, 238–250.
[52] Eisele, J.-L. and Rosenbusch, J.P. (1990) J. Biol. Chem. 265, 10217–10220.
[53] Engelman, D.M., Steiz, T.A. and Goldman, A. (1986) Annu. Rev. Biophys. Biophys. Chem. 15, 321–353.
[54] Engelman, D.M., Adair, B.D., Hunt, J.F., Kahn, T.W. and Popot, J.-L. (1990) Curr. Topics Membr. Transport 36, 71–78.
[55] Ermler, U., Michel, H. and Schiffer, M. (1994) J. Bioenerget. Biomembr. 26, 5–15.
[56] Finbow, M.E., Eliopoulos, E.E., Jackson, P.J., Keen, J.N., Meagher, L., Thompson, P., Jones, P. and Findlay, J.B.C. (1992) Protein Eng. 5, 7–15.
[57] Fischbarg, J., Cheung, M., Czegledy, F., Li, J., Iserovich, P., Kuang, K., Hubbard, J., Garner, M., Rosen, O.M., Golde, D.W. and Vera, J.C. (1993) Proc. Natl. Acad. Sci. USA 90, 11658–11662.
[58] Franklin, J.C. and Cafiso, D.S. (1993) Biophys. J. 65, 289–299.
[59] Freire, E., Haynie, D.T. and Xie, D. (1993) Proteins 17, 111–123.
[60] Gawrisch, K., Ruston, D., Zimmerberg, J., Parsegian, V.A., Rand, R.P. and Fuller, N. (1992) Biophys. J. 61, 1213–1223.
[61] Groves, J.D. and Tanner, M.J.A. (1992) J. Biol. Chem. 267, 22163–22170.
[62] Groves, J.D., Ring, S.M., Schofield, A.E. and Tanner, M.J.A. (1993) FEBS Lett. 330, 186–190.
[63] Fonseca, V., Daumas, P., Ranjalahy-Rasoloarijao, L., Heiz, F., Lazaro, R., Trudelle, Y. and Andersen, O.S. (1992) Biochemistry 31, 5340–5350.
[64] Frey, T.G. and Murray, J.M. (1994) J. Mol. Biol. 237, 275–297.
[65] Fuhrtmayr, H. and Marchesi, V.T. (1976) Biochemistry 31, 1137–1144.
[66] Galisteo, M.L. and Sanchez-Ruiz, J.M. (1993) Eur. Biophys. J. 22, 25–30.
[67] Garcia-Horsman, J.A., Berry, E.A., Shapleigh, J.P., Alben, J.O. and Gennis, R.B. (1994) Biochemistry 33, 3113–3119.
[68] Gennis, R.B. (1989) Biomembranes–Molecular Structure and Function, Springer, New York.
[69] Gilles-Gonzalez, M.A., Engelman, D.M. and Khorana, H.G. (1991) J. Biol. Chem. 266, 8545–8550.
[70] Gilson, M.K. and Honig, B. (1989) Proc. Natl. Acad. Sci. USA 86, 1524–1528.
[71] Görne-Tschelnokow, U., Strecker, A., Kaduk, C., Naumann, D. and Hucho, F. (1994) EMBO J. 13, 338–341.
[72] Gray, K A., Grooms, M., Myllykallio, H., Moomaw, C., Slaughter, C. and Daldal, F. (1994) Biochemistry 33, 3120–3127.
[73] Greenhalgh, D.A., Farrens, D.L., Subramaniam, S. and Khorana, H.G. (1993) J. Biol. Chem. 268, 20305–20311.
[74] Haltia, T. and Wikström, M. (1992) in Molecular Mechanisms in Bioenergetics (Ernster, L., ed.), New Compherensive Biochemistry, Vol. 23, pp. 217–239, Elsevier, Amsterdam.
[75] Haltia, T., Finel, M., Harms, N., Nakari, T., Raitio, M., Wikström, M. and Saraste, M. (1989) EMBO J. 8, 3571–3579.
[76] Haltia, T., Saraste, M. and Wikström, M. (1991) EMBO J. 10, 2015–2021.

[77] Haltia, T., Semo, N., Arrondo, J.L.R., Goni, F.M. and Freire, E. (1994) Biochemistry 33, 9731–9740.
[78] Havelka, W.A., Henderson, R., Heymann, J.A.W. and Oesterhelt, D. (1993) J. Mol. Biol. 234, 837–846.
[79] Haynie, D.T. and Freire, E. (1993) Proteins 16, 115–140.
[80] Henderson, R., Baldwin, J.M., Ceska, T.M., Zemlin, F., Beckmann, E. and Downing, K.H. (1990) J. Mol. Biol. 213, 899–929.
[81] Hendler, R.W., Pardhasaradhi, K., Reynafarje, B. and Ludwig, B. (1991) Biophys. J. 60, 415–423.
[82] Honig, B.H. and Hubbel, W.L. (1984) Proc. Natl. Acad. Sci. USA 81, 5412–5416.
[83] Honig, B.H., Hubbel, W.L. and Flewelling, R.F. (1986) Annu. Rev. Biophys. Biophys. Chem. 15, 163–193.
[84] Hosler, J.P., Ferguson-Miller, S., Calhoun, M.W., Thomas, J.W., Hill, J., Lemieux, L., Ma, J., Georgiou, C., Fetter, J., Shapleigh, J., Tecklenburg, M.M.J., Babcock, G.T. and Gennis, R.B. (1993) J. Bionerget. Biomembr. 25, 131–136.
[85] Hill, B.C., Cook, K. and Robinson, N.C. (1988) Biochemistry 27, 4741–4747.
[86] Hu, W., Lee, K.-C. and Cross, T.A. (1993) Biochemistry 32, 7035–7047.
[87] Huang, K.-S., Bayley, H., Liao, M.-J., London, E. and Khorana, H.G. (1981) J. Biol. Chem. 256, 3802–3809.
[88] Hunter, C.N., Artymiuk, P.J. and van Amerongen, H. (1994) Curr. Biol. 4, 344– 346.
[89] Ishizuka, M., Machida, K., Shimada, S., Mogi, A., Tsuchiya, T., Ohmori, T., Souma, Y., Gonda, M. and Sone, N. (1990) J. Biochem. 220, 57–66.
[90] Jackson, M.B. and Sturtevant, J.M. (1978) Biochemistry 17, 911–915.
[91] Jarolim, P., Palek, J., Amato, D., Hassan, K., Sapak, P., Nurse, G.T., Rubin, H.L., Zhai, S., Sahr, K.E. and Liu, S.-C. (1991) Proc. Natl. Acad. Sci. USA 88, 11022– 11026.
[92] Jennings, M.L. (1989) Annu. Rev. Biochem. 58, 999–1027.
[93] Jones, D.T., Taylor, W.R. and Thornton, J.M. (1994) FEBS Lett. 339, 269–275.
[94] Jones, D.T., Taylor, W.R. and Thornton, J.M. (1994) Biochemistry 33, 3038–3049.
[95] Kaback, H.R., Jung, K., Jung, H., Wu, J., Prive, G. and Zen, K. (1993) J. Bioenerget. Biomembr. 25, 627–636.
[96] Kahn, T.W. and Engelman, D.M. (1992) Biochemistry 31, 6144–6151.
[97] Kahn, T.W., Sturtevant, J.M. and Engelman, D.M. (1992) Biochemistry 31, 8829–8839.
[98] Kates, M., Kushawa, S.C. and Sprott, G.D. (1982) Methods Enzymol. 88, 98–111.
[99] Ketchem, R.R., Hu, W. and Cross, T.A. (1993) Science 261, 1457–1460.
[100] Komiya, H., Yeates, T.O., Rees, D.C., Allen, J.P. and Feher, G. (1988) Proc. Natl. Acad. Sci. 85, 9012–9016.
[101] Kraulis, P. (1991) J. Appl. Crystallogr. 24, 946–950.
[102] Krauss, N., Hinrichs, W., Witt, I., Fromme, P., Pritzkow, W., Dauter, Z., Betzel, C., Wilson, K.S., Witt, H.S. and Sanger, W. (1993) Nature 361, 326–331.
[103] Krebs, M.P. and Khorana, H.G. (1993) J. Bacteriol. 175, 1555–1560.
[104] Kreusch, A., Neubüser, A., Schilz, E., Weckesser, J. and Schulz, G.E. (1994) Protein Sci. 3, 58–63.
[105] Kühlbrandt, W., Wang, D.N. and Fujiyoshi, Y. (1994) Nature 367, 614–621.
[106] Landolt-Marticorena, C., Williams, K.A., Deber, C.M. and Reithmeier, R.A.F. (1993) J. Mol. Biol. 229, 602–608.
[107] Lappalainen, P., Aasa, R., Malmström, B.G. and Saraste, M. (1993) J. Biol. Chem. 268, 26416–26421.
[108] Lee, J.-I., Hwang, P.P. and Wilson, T.H. (1993) J. Biol. Chem. 268, 20007–20015.
[109] Lee, K.H., Xie, D., Freire, E. and Amzel, L.M. (1994) Proteins, 20, 68–84.
[110] Lemmon, M.A. and Engelman, D.M. (1992) Curr. Opin. Struct. Biol. 2, 511–518.
[111] Lemmon, M.A., Flanagan, J.M., Hunt, J.F., Adair, B.D., Bormann, B.J., Dempsey, C.E. and Engelman, D.M. (1992) J. Biol. Chem. 267, 7683–7689.
[112] Lemmon, M.A., Flanagan, J.M., Treutlein, H.R., Zhang, J. and Engelman, D.M. (1992) Biochemistry 31, 12719–12725.
[113] Lemmon, M.A., Treutlein, H.R., Adams, P.D., Brünger, A.T. and Engelman, D.M. (1994) Nature Struct. Biol. 1, 157–163.
[114] Lepke, S., Becker, A. and Passow, H. (1992) Biochim. Biophys. Acta 1106, 13–16.
[115] Liao, M.-J., London, E. and Khorana, H.G. (1983) J. Biol. Chem. 258, 9949–9955.
[116] Liao, M.-J., Huang, K.-S. and Khorana, H.G. (1984) J. Biol. Chem. 259, 4200–4204.
[117] Lodish, H.F. (1988) Trends Biochem. Sci. 13, 332–334.
[118] Lübben, M., Kolmerer, B. and Saraste, M. (1992) EMBO J. 11, 805–812.
[119] Lynch, B.A. and Koshland, D.E. Jr. (1991) Proc. Natl. Acad. Sci. USA 88, 10402– 10406.
[120] Ma, J., Lemieux, L. and Gennis, R.B. (1993) Biochemistry 32, 7692–7697.
[121] Malik, S., Sami, M. and Watts, A. (1993) Biochemistry 32, 10078–10084.
[122] Malmström, B.G. (1993) Acc. Chem. Res. 26, 332–338.
[123] Maneri, L.R. and Low, P.S. (1988) J. Biol. Chem. 263, 16170–16178.
[124] Manolios, N., Bonifacino, J.S. and Klausner, R.D. (1990) Science 249, 274–277.
[125] Martinez, S.E., Huang, D., Szczepaniak, A., Cramer, W.A. and Smith, J.L. (1994) Structure 2, 95–105.
[126] Mather, M.W., Springer, P., Hensel, S., Buse, G. and Fee, J.A. (1993) J. Biol. Chem. 268, 5395–5408.
[127] Michel, H., Weyer, K.A., Gruenberg, H., Dunger, I., Oesterhelt, D. and Lotspeich, F. (1986) EMBO J. 5, 1149–1158.
[128] Michel, H. and Deisenhofer, J. (1990) Curr. Topics Membr. Transport 36, 53–78.
[129] Milburn, M.V., Prive, G.G., Milligan, D.L., Scott, W.G., Yeh, J., Jancarik, J., Koshland, D.E. and Kim, S.-H. (1991) Science 254, 1342–1347.
[130] Millar, D.G. and Shore, G.C. (1994) J. Biol. Chem. 269, 12229–12232.
[131] Mogi, T., Marti, T. and Khorana, H.G. (1989) J. Biol. Chem. 264, 14197–14201.
[132] Mohandas, N., Windari, R., Knowles, D., Leung, A., Parra, M., George, E., Conboy, J. and Chasis, J. (1992) J. Clin. Invest. 89, 686–692.
[133] Morin, P.E. and Freire, E. (1991) Biochemistry 30, 8494–8500.
[134] Morin, P.E., Diggs, D. and Freire, E. (1990) Biochemistry 29, 781–788.
[135] Moriyama, R., Ideguchi, H., Lombardo, C.R., Van Dort, H.M. and Low, P.S. (1992) J. Biol. Chem. 267, 25792–25797.
[136] Mouritsen, O.G. and Sperotto, M.M. (1993) in Thermodynamics of Membrane Receptors and Channels (Jackson, M.B., ed.), pp. 127–181, CRC Press, Boca Raton, FL.
[137] Murphy, K.P., Bhakuni, V., Xie, D. and Freire, E. (1992) J. Mol. Biol. 227, 293–306.
[138] Murphy, K.P. and Freire, E. (1992) Adv. Protein Chem. 43, 313–361.
[139] Murphy, K.P., Privalov, P.L. and Gill, S.J. (1990) Science 247, 559–561.
[140] Nagle, J.F. and Wilkinson, D.A. (1978) Biophys. J. 23, 159–175.
[141] Nemethy, G., Leach, S.J. and Scheraga, H.A. (1966) J. Phys. Chem. 70, 998–1004.

[142] Nikaido, H. (1992) Mol. Microbiol. 6, 435–442.
[143] Nikaido, H. (1994) J. Biol. Chem. 269, 3905–3908.
[144] Nikaido, H. and Reid, J. (1990) Experientia 46, 174–180.
[145] Nussberger, S., Dörr, K., Wang, D.N. and Kühlbrandt, W. (1993) J. Mol. Biol. 234, 347–356.
[146] Oikawa, K., Lieberman, D.M. and Reithmeier, R.A.F. (1985) Biochemistry 24, 2843–2848.
[147] Pakrasi, H.B., De Ciechi, P. and Whitmarsh, J. (1991) EMBO J. 10, 1619–1627.
[148] Pakula, A.A. and Simon, M.I. (1992) Proc. Natl. Acad. Sci. USA 89, 4144–4148.
[149] Park, K., Perczel, A. and Fasman, G.D. (1992) Protein Sci. 1, 1032–1049.
[150] Persson, B. and Argos, P. (1994) J. Mol. Biol. 237, 182–192.
[151] Plumley, F.G. and Schmidt, G.W. (1987) Proc. Natl. Acad. Sci. USA 84, 146–150.
[152] Ponnuswamy, P.K. and Gromiha, M.M. (1993) Int. J. Peptide Protein Res. 42, 326– 341.
[153] Picot, D., Loll, P.J. and Garavito, R.M. (1994) Nature 367, 243–249.
[154] Pongs, O. (1993) J. Membr. Biol. 136, 1–8.
[155] Popot, J.-L. (1993) Curr. Opin. Struct. Biol. 3, 532–540.
[156] Popot, J.-L. and De Vitry, C. (1990) Annu. Rev. Biophys. Biophys. Chem. 19, 369–403.
[157] Popot, J.-L. and Engelman, D.M. (1990) Biochemistry 29, 4031–4037.
[158] Popot, J.-L., Gerchmann, S.E. and Engelman, D.M. (1987) J. Mol. Biol. 198, 655– 676.
[159] Preisig, O., Anthamatten, D. and Hennecke, H. (1993) Proc. Natl. Acad. Sci. USA 90, 3309–3313.
[160] Privalov, P.L. and Gill, S.J. (1988) Adv. Protein Chem. 39, 191–234.
[161] Privalov, P.L. and Makhatadze, G.I. (1993) J. Mol. Biol. 232, 660–679.
[162] Quirk, P.G., Hicks, D.B. and Krulwich, T.A. (1993) J. Biol. Chem. 268, 678–685.
[163] Rees, D.C., DeAntonio, L. and Eisenberg, D. (1989) Science 245, 510–513.
[164] Rees, D.C., Komiya, H., Yeates, T., O., Allen, J.P. and Feher, G. (1989) Annu. Rev. Biochem. 58, 607–633.
[165] Reithmeier, R.A.F. (1993) Curr. Opin. Struct. Biol. 3, 515–523.
[166] Renthal, R. (1992) in Molecular Mechanisms in Bioenergetics (Ernster, L., ed.), New Compherensive Biochemistry, Vol. 23, pp. 75–101, Elsevier, Amsterdam.
[167] Richards, F. (1977) Annu. Rev. Biophys. Bioeng. 6, 151–176.
[168] Rigell, C., De Saussure, C. and Freire, E. (1985) Biochemistry 24, 5638–5646.
[169] Rigell, C. and Freire, E. (1987) Biochemistry 26, 4366–4371.
[170] Robinson, N.C. (1993) J. Bioenerget. Biomembr. 25, 153–163.
[171] Roth, M., Lewit-Bentley, A., Michel, H., Deisenhofer, J., Huber, R. and Oesterhelt, D. (1989) Nature 340, 659–661.
[172] Roth, M., Arnoux, B. and Reiss-Husson, F. (1991) Biochemistry 30, 9403–9413.
[173] Rothschild, K.J., Marti, T., Sonar, S., He, Y.-W., Rath, P., Fischer, W. and Khorana, H.G. (1993) J. Biol. Chem. 268, 27046–27052.
[174] Rutledge, T., Cosson, P., Manolios, N., Bonifacino, J.S. and Klausner, R.D. (1992) EMBO J. 11, 3245–3254.
[175] Sahin-Toth, M. and Kaback, H.R. (1993) Biochemistry 32, 10027–10035.
[176] Salhany, J.M., Cordes, K.A. and Schopfer, L.M. (1993) Biochemistry 32, 7413–7420.
[177] Sami, M., Malik, S. and Watts, A. (1992) Biochim. Biophys. Acta 1105, 148–154.
[178] Sarabia, V.E., Casey, J.R. and Reithmeier, R.A.F. (1993) J. Biol. Chem. 268, 10676–10680.
[179] Saraste, M. (1990) Q. Rev. Biophys. 23, 331–366.
[180] Saraste, M. and Castresana, J. (1994) FEBS Lett. 341, 1–4.
[181] Schertler, G.F.X., Villa, C. and Henderson, R. (1993) Nature 362, 770–772.
[182] Schiffer, M., Chang, C.-H. and Stevens, F.J. (1992) Protein Eng. 5, 213–214.
[183] Schilz, E., Kreusch, A., Nestel, U. and Schulz, G.E. (1991) Eur.J. Biochem. 199, 587–594.
[184] Schirmer, T. and Cowan, S.W. (1993) Protein Sci. 2, 1361–1363.
[185] Schofield, A.E., Reardon, D.M. and Tanner, M.J.A. (1992) Nature 355, 836–838.
[186] Schofield, A.E., Tanner, M.J.A., Pinder, J.C., Clough, B., Bayley, P.M., Nash, G.B., Dluzewski, A.R., Reardon, D.M., Cox, T.M., Wilson, R.J.M. and Gratzer, W.B. (1992) J. Mol. Biol. 223, 949–958.
[187] Schultz, G.E. (1992) in Membrane Proteins: Structures, Interactions and Models (Pullman, A., Jortner, J. and Pullman, B., eds.), pp. 403–412, Kluwer Academic, Dordrecht.
[188] Schulz, G.E. (1993) Curr. Opin. Cell Biol. 5, 701–707.
[189] Scott, W.G., Milligan, D.L., Milburn, M.V., Prive, G.G., Yeh, J., Koshland, D.E. and Kim, S.-H. (1993) J. Mol. Biol. 232, 555–573.
[190] Semin, B.K., Saraste, M. and Wikström, M. (1984) Biochim. Biophys. Acta 769, 15– 22.
[191] Shnyrov, V.L. and Mateo, P.L. (1993) FEBS Lett. 324, 237–240.
[192] Sigrist, H., Wenger, R.H., Kislig, E. and Wütrich, M. (1988) Eur. J. Biochem. 177, 125–133.
[193] Singer, S.J. (1990) Annu. Rev. Cell Biol. 6, 247–296.
[194] Sipos, L. and Von Heijne, G. (1993) Eur. J. Biochem. 213, 1333–1340.
[195] Sixma, T.K., Pronk, S.E., Kalk, K.H., Wartna, E.S., Van Zanten, B.A.M., Witholt, B. and Hol, W.G.J. (1991) Nature 351, 371–377.
[196] Snow, J.W., Brandts, J.F. and Low, P.S. (1978) Biochim. Biophys. Acta 512, 579– 591.
[197] Snow, J.W., Vincentelli, J. and Brandts, J.F. (1981) Biochim. Biophys. Acta 642, 418–428.
[198] Stein, P.E., Boodhoo, A., Tyrrell, G.J., Brunton, J.L. and Read, R.J. (1992) Nature 355, 748–750.
[199] Stern, L.J. and Khorana, H.G. (1989) J. Biol. Chem. 264, 14202–14208.
[200] Sternberg, B., L'Hostis, C., Whiteway, C.A. and Watts, A. (1992) Biochim. Biophys. Acta 1108, 21–30.
[201] Sternberg, B., Watts, A. and Cejka, Z. (1993) J. Struct. Biol. 110, 196–204.
[202] Sternberg, M.J.E. (1990) Protein Eng. 4, 45–47.
[203] Sternberg, M.J.E. and Gullick, W.J. (1989) Nature 339, 587.
[204] Sternberg, M.J.E. and Gullick, W.J. (1990) Protein Eng. 3, 245–248.
[205] Steverding, D., Köhnke, D., Ludwig, B. and Kadenbach, B. (1993) Eur. J. Biochem. 212, 827–831.
[206] Solioz, M., Carafoli, E. and Ludwig, B. (1982) J. Biol. Chem. 257, 1579–1582.
[207] Subramaniam, S., Gerstein, M., Oesterhelt, D. and Henderson, R. (1993) EMBO J. 12, 1–8.
[208] Tanner, H.J.A. (1989) Methods Enzymol. 173, 423–432.
[209] Tanner, M.J.A. (1993) Sem. Hematol. 30, 34–57.
[210] Taylor, W.R., Jones, D.T. and Green, N.M. (1994) Proteins 18, 281–294.
[211] Teufel, M., Pompejus, M., Humbel, B., Friedrich, K., and Fritz, H.-J. (1993) EMBO J. 12, 3399–3408.
[212] Thompson, L.K., Sturtevant, J.M. and Brudwig, G.W. (1986) Biochemistry 25, 6161–6169.
[213] Thompson, L.K., Blaylock, R., Sturtevant, J.M. and Brudwig, G.W. (1989) Biochemistry 28, 6686–6695.
[214] Toyoshima, C., Sasabe, H. and Stokes, D.L. (1993) Nature 362, 469–471.
[215] Traxler, B., Boyd, D. and Beckwith, J. (1993) J. Membr. Biol. 132, 1–11.
[216] Treutlein, H.R., Lemmon, M.A., Engelman, D.M. and Brünger, A.T. (1992) Biochemistry 31, 12726–12733.

[217] Tuffery, P., Etchebest, C., Popot, J.-L. and Lavery, R. (1994) J. Mol. Biol. 236, 1105– 1122.
[218] Unwin, N. (1993) J. Mol. Biol. 229, 1101–1124.
[219] Valpuesta, J.M., Henderson, R. and Frey, T.G. (1990) J. Mol. Biol. 214, 237–251.
[220] Van der Oost, J., Musacchio, A., Pauptit, R.A., Ceska, T.A., Wierenga, R.K. and Saraste, M. (1993) J. Mol. Biol. 229, 794–796.
[221] Van der Oost, J., De Boer, A.P.N., De Gier, J.-W.l., Zumft, W.G., Stouthamer, A.H. and Van Sapnning, R.J.M. (1994) Microbiol. Lett. 121, 1–10.
[222] Van Dort, H.M., Low, P.S., Cordes, K.A., Schopfer, L.M. and Salhany, J.M. (1994) J. Biol. Chem. 269, 59–61.
[223] Von Heijne, G. (1986) EMBO J. 5, 3021–3027.
[224] Von Heijne, G. (1988) Biochim. Biophys. Acta 947, 307–333.
[225] Von Heijne, G. (1991) J. Mol. Biol. 218, 499–503.
[226] Von Heijne, G. (1992) J. Mol. Biol. 225, 487–494.
[227] Von Heijne, G. and Gavel, Y. (1988) Eur. J. Biochem. 174, 671–678.
[228] Von Heijne, G. and Manoil, C. (1990) Protein Eng. 4, 109–112.
[229] Wang, C.C., Badylak, J.A., Lux, S.E., Moriyama, R., Dixon, J.E. and Low, P.S. (1992) Protein Sci. 1, 1206–1214.
[230] Wang, D.N., Kühlbrandt, W., Sarabia, V.E. and Reithmeier, R.A.F. (1993) EMBO J. 12, 2233–2239.
[231] Wang, J. and Pullman, A. (1991) Biochim. Biophys. Acta 1070, 493–496.
[232] Wess, J., Nanavati, S., Vogel, Z. and Maggio, R. (1993) EMBO J. 12, 331–338.
[233] Weiss, M.S. and Schulz, G.E. (1992) J. Mol. Biol. 227, 493–509.
[234] Weiss, M.S., Abele, U., Weckesser, J., Welte, W., Schilz, E. and Schulz, G.E. (1991) Science 254, 1627–1630.
[235] White, S.H. and Jacobs, R.E. (1990) J. Membr. Biol. 115, 145–158.
[236] White, S.H. and Wimley, S.H. (1994) Curr. Opin. Struct. Biol. 4, 79–86.
[237] Whitley, P., Nilsson, L. and Von Heijne, G. (1993) Biochemistry 32, 8534–8539.
[238] Wiener, M.C. and White, S.H. (1992) Biophys. J. 61, 434–447.
[239] Williams, K.A. and Deber, C.M. (1991) Biochemistry 30, 8919–8923.
[240] Wimley, W.C. and White, S.H. (1993) Biochemistry 32, 6307–6312.
[241] Woese, C.R. (1979) J. Mol. Evol. 13, 95–101.
[242] Woese, C.R. (1987) Microbiol. Rev. 51, 227–271.
[243] Woolley, G.A. and Wallace, B.A. (1993) Biochemistry 32, 9819–9825.
[244] Yeates, T. (1993) in Thermodynamics of Membrane Receptors and Channels (Jackson, M.B., ed.), pp. 1–25, CRC Press, Boca Raton, FL.
[245] Yu, C.A., Gwak, S.H. and Yu, L. (1985) Biochim. Biophys. Acta 812, 656–664.
[246] Bormann, B.J. and Engelman, D.M. (1992) Annu. Rev. Biophys. Biomol. Struct. 21, 223–242
[247] Mielke, D.L. and Wallace, B.A. (1988) J. Biol. Chem. 263, 3177–3182.
[248] Xie, D. and Freire, E. (1994) Proteins 19, 291–301.
[249] Dneber, C.M., Khan, A.R., Li, Z., Joensson, C., Glibowicka, M. and Wang, J. (1993) Proc. Natl. Acad. Sci. USA 90, 11648–11652.
[250] Zhang, Y.-P., Lewis, R.N.A.H., Hodges, R.S. and McElhaney, R.N. (1992) Biochemistry 31, 11572–11578.
[251] Ghadiri, M.R., Granja, J.R. and Buehler, L.K. (1994) Nature 369, 301–304.
[252] Sun, S. and Parthasarathy, R. (1994) Biophys. J. 66, 2092–2106.
[253] Lemmon, M.A. and Engelman, D.M. (1994) FEBS Lett. 346, 17–20.
[254] Wang, D.N. (1994) FEBS Lett. 346, 26–31.
[255] Picot, D. and Garavito, R.M. (1994) FEBS Lett. 346, 21–25.
[256] Stokes, D.L., Taylor, W.R. and Green, N.M. (1994) FEBS Lett. 346, 32–38.
[257] Frey, T.G. (1994) Microsc. Res. Tech. 27, 319–332.
[258] Hobe, S. Prytulla, S., Kühlbrandt, W. and Paulsen, H. (1994) MEBO J. 13, 3423–3429.
[259] Montoya, G., Cases, R. Rodriguez, R., Aured, M. and Picorel, R. (1994) Biochemistry 33, 11798–11804.